European Journal of Taxonomy 573: 1–38
https://doi.org/10.5852/ejt.2019.573
ISSN 2118-9773
www.europeanjournaloftaxonomy.eu
2019 · Coughlan K. & Stec D.



**Research article**

urn:lsid:zoobank.org:pub:7619772F-2300-442E-8950-69559172360E

# Two new species of the *Macrobiotus hufelandi* complex (Tardigrada: Eutardigrada: Macrobiotidae) from Australia and India, with notes on their phylogenetic position

Kyle COUGHLAN [1] & Daniel STEC [2,*]

[1,2] Institute of Zoology and Biomedical Research, Jagiellonian University, Gronostajowa 9, 30-387 Kraków, Poland.

[*] Corresponding author: daniel_stec@interia.eu
[1] Email: kyle.coughlan@doctoral.uj.edu.pl

[1] urn:lsid:zoobank.org:author:8462AE94-14E5-4280-AA96-DB9101F3D4DE
[2] urn:lsid:zoobank.org:author:13C435F8-25AB-47DE-B5BB-8CE788E92CF6

**Abstract.** In this paper we describe two new tardigrade species belonging to the *Macrobiotus hufelandi* complex: *Macrobiotus noongaris* sp. nov. from Perth, Australia, and *Macrobiotus kamilae* sp. nov. from Mussoorie, India. Live specimens extracted from moss samples were used to establish laboratory cultures in order to obtain additional animals and eggs needed for their integrative descriptions. These descriptions are based on traditional morphological and morphometric data collected using both light and scanning electron microscopy, which, at the same time, were associated with DNA sequences of four genetic markers, three nuclear (18S rRNA, 28S rRNA and ITS-2) and one mitochondrial (COI). The use of DNA sequences allowed for a more accurate verification of the taxonomic status of *M. noongaris* sp. nov. and *M. kamilae* sp. nov as independent species of the *hufelandi* group. Although they both exhibit typical inverted goblet-shaped processes, they represent a recently discovered clade, which was thought to group species with modified morphology of egg processes. Thus, this contribution expands the definition of the mentioned clade and constitutes another link that will be helpful for future studies on the evolution of the *M. hufelandi* complex.

**Key words.** Egg ornamentation, Indian Himalayas, species complex, taxonomy, Western Australia.

Coughlan K. & Stec D. 2019. Two new species of the *Macrobiotus hufelandi* complex (Eutardigrada: Macrobiotidae) from Australia and India, with notes on their phylogenetic position. *European Journal of Taxonomy* 573: 1–38. https://doi.org/10.5852/ejt.2019.573

## Introduction

Tardigrades, also known as water bears or moss piglets, are a phylum of micrometazoans closely related to arthropods and onychophorans, although their exact placement within the Ecdysozoa remains unclear (Campbell *et al.* 2011). Since their discovery in the 18th century by the German zoologist Johan Goeze, nearly 1300 species have been described (Guidetti & Bertolani 2005; Degma & Guidetti 2007; Degma *et al.* 2009–2019). Tardigrades have a global distribution and can be found in both marine and terrestrial

habitats. However, most of the described species have been discovered from mosses and lichen, where at least periodic hydration is required in order for them to survive. They have been found to exist in the most extreme environments on Earth, from the ocean depths to mountain tops and are present in all biomes and on every continent including Antarctica (Nelson *et al.* 2015).

Here, we describe two species within the *Macrobiotus hufelandi* group, a species complex considered to be among the most common group of limnoterrestrial tardigrades on the planet (Bertolani & Rebecchi 1993; McInnes 1994; Kaczmarek *et al.* 2014a, 2015, 2016; Kaczmarek & Michalczyk 2017a; McInnes *et al.* 2017). *Macrobiotus hufelandi* Schultze, 1834 was the first ever formally described tardigrade species, and for over a century this species was believed to be cosmopolitan, but also exhibited some intraspecific variability. Subsequently, the discovery of very similar species, such as *Macrobiotus hibiscus* de Barros, 1942 and several more over the next three decades, led to the introduction of the term "*Macrobiotus hufelandi* group" which was first used by Durante Pasa & Maucci (1979), with Biserov (1990a, 1990b) as the first to attempt to formally define the *Macrobiotus hufelandi* group. A revision of the criteria for inclusion in the *hufelandi* group by Bertolani & Rebecchi (1993), along with a redescription of the nominal species, listed 17 species contained within this species complex. The most recent revision of the group, Kaczmarek & Michalczyk (2017a), recorded 48 species and predicted at least six more to be described by 2020, a prediction which has already been surpassed. To date six formal descriptions of new species within the *hufelandi* complex have been published and with this paper we add two more. The six others are *Macrobiotus nebrodensis* Pilato, Sabella, D'Urso & Lisi, 2017 from Italy, *M. canaricus* Stec, Krzywański & Michalczyk, 2018 from the Canary Islands, *M. papei* Stec, Kristensen & Michalczyk, 2018 from Tanzania, *M. hannae* Nowak & Stec, 2018 from Poland, *M. shonaicus* Stec, Arakawa & Michalczyk, 2018 from Japan, *M. dulciporus* Roszkowska, Gawlak, Draga & Kaczmarek, 2019 from Ecuador and *M. noemiae* Roszkowska & Kaczmarek, 2019 from Spain. The majority of these descriptions were prepared by means of integrative taxonomy, which together with previous integrative studies on the *M. hufelandi* complex (Guidetti *et al.* 2005; Cesari *et al.* 2009; Bertolani *et al.* 2011a, 2011b; Guidetti *et al.* 2013) have enabled for the first time more detailed insights into the evolution of this eutardigrade group. Specifically, Stec *et al.* (2018a, 2018b) discovered two well supported evolutionary lineages within this complex. This diversification was also congruent with morphology, since one of the discovered clades comprised species with a whitish body and mostly typical inverted goblet shaped processes, whereas the second one comprised species with a yellowish body and eggs with processes having a modified morphology.

Although the first studies of Indian tardigrades were conducted as early as in the beginning of the 20$^{th}$ century (Murray 1907) and again in the second part of the century (Iharos 1969), very little is known about the terrestrial tardigrade fauna of the Indian subcontinent. Tumanov (2018) listed only eight published papers on the subject, including the two mentioned above, but also noted that these "should be considered obsolete compared to the current levels of morphological data on this taxon". Apart from larger studies based on islands far from the Indian mainland such as Maucci & Durante Pasa (1980) and Roa (1972), the other published studies, namely Maucci (1979), Kristensen (1987), Abe & Takeda (2000), Tumanov (2006, 2018) and Jørgensen *et al.* (2007), are based on data for single species obtained mostly from solitary samples collected occasionally. A review study conducted as part of the Zoological survey of India counted 41 species of tardigrades known to India, with 23 species listed as being found in the Indian Himalaya (Dey & Mandal 2018). Although that study listed *M. hufelandi hufelandi* as being present in India, considering the immense progress in our understanding of the diversity and taxonomy of the *hufelandi* group made since the Indian record by Murray (1907), this record most likely represents a different species.

In contrast to India, the tardigrade fauna of Australia has been much more studied through the years with early expeditions being undertaken by Richters (1908), who observed *M. hufelandi* in the Blue

Mountains (again, most likely a different species in the group), and Murray (1910) who recorded 31 species (including 6 new to science) in the states of New South Wales and Queensland. Notably, however, in the *hufelandi* complex only two species have previously been described from Australia, namely *Macrobiotus joannae* Pilato & Binda, 1983 from Bright in the state of Victoria and *M. santoroi* Pilato & D'Urso, 1976 from near Sydney in the state of New South Wales. With regard to tardigrade diversity in Australia, the largest study undertaken to date was that of Claxton (2004) as part of her Ph.D. thesis, in which she found 141 species from 132 samples collected in Eastern Australia. Two other papers are, however, of particular relevance as they pertain to tardigrade species found in Western Australia, specifically around the city of Perth, where the first of the new species described below has been found. Morgan & Nicholls (1986) described *Apodibius serventyi* from moss samples collected in the Perth Zoo, which was later considered as a synonym of *A. nuntius* Binda, 1984 (Van Rompu *et al.* 1995). A re-examination of the slides with 'types' of *A. serventyi* by Pilato & Lisi (2004) led to the discovery and description of two additional species, *Doryphoribius neglectus* Pilato & Lisi, 2004 and *Parascon nichollsae* Pilato & Lisi, 2004. An additional study by Gąsiorek & Michalczyk (2019) described *Echiniscus siticulosus* discovered in Western Australia, albeit it from an area 650 km to the north of Perth.

This study combines modern molecular techniques with classical morphometric and morphological methods in an integrative approach to describe two new species within the *M. hufelandi* complex. Using phase contrast and scanning electron microscopy (PCM and SEM, respectively), we have described the phenotypic characteristics of the new species, whereas the sequencing of DNA markers (three nuclear, 18S rRNA, 28S rRNA and ITS-2, and one mitochondrial, COI) allowed for an assessment of the phylogenetic position of the new species within the *M. hufelandi* complex and also provided barcodes for their genetic identification.

## Material and methods

### Sample processing and tardigrade culturing

One of the two moss samples analysed in this study was collected from King's Park, an urban park of bushland in the city of Perth situated in the state of Western Australia, Australia (31°57′30″ S, 115°50′09″ E). The moss was growing on soil at an altitude of 46 m a.s.l. and was collected on 22 March 2015 by Łukasz Michalczyk. The second sample of moss was collected from an urban area along Camel's Back Road in the town of Mussoorie in the Dehradin District of the state of Uttarakhand, India, which is situated at the foothills of the Garhwal Himalayan mountain range (30°27′28″ N, 78°04′41″ E). The moss was growing on rock at an altitude of 2001 m a.s.l. and was collected on 10 November 2017 by Krzysztof Miller.

The samples were examined for tardigrades using the protocol by Dastych (1980) with modifications described in detail in Stec *et al.* (2015). A total of 13 and 28 live individuals and no eggs of the new species were extracted from the Australian and Indian samples, respectively. They were subsequently used to establish laboratory cultures to obtain additional animals and eggs for further analysis. Tardigrades were reared in plastic Petri dishes according to the protocol by Stec *et al.* (2015) and are still maintained in the lab culture. In order to perform the taxonomic analysis, animals and eggs were isolated from the culture and split into three groups for specific analyses: morphological analysis with phase contrast light microscopy, morphological analysis with scanning electron microscopy and DNA sequencing (for details, please see section "Material examined" provided below for each description).

### Microscopy and imaging

Specimens for light microscopy were mounted on microscope slides in a small drop of Hoyer's medium and secured with a cover slip, following the protocol by Morek *et al.* (2016). Slides were examined under an Olympus BX53 light microscope with phase contrast (PCM), associated with an Olympus

DP74 digital camera. Subsequently, after mounting, the specimens in the medium slides where also checked under PCM for the presence of males and females in the studied population, as the spermatozoa in testis and spermathecae are visible for several hours after mounting. In order to obtain clean and extended specimens for SEM, tardigrades were processed according to the protocol of Stec *et al.* (2015). Specimens were examined under high vacuum in a Versa 3D DualBeam Scanning Electron Microscope (SEM) at the ATOMIN facility of the Jagiellonian University, Kraków, Poland. All figures were assembled in Corel Photo-Paint X6, ver. 16.4.1.1281. For structures that could not be satisfactorily focused in a single light microscope photograph, a stack of 2–6 images were taken with an equidistance of ca 0.2 µm and assembled manually into a single deep-focus image in Corel Photo-Paint X6, ver. 16.4.1.1281.

### Morphometrics and morphological nomenclature

All measurements are given in micrometres (µm). Sample size was adjusted following recommendations by Stec *et al.* (2016a). Structures were measured only if their orientation was suitable. Body length was measured from the anterior extremity to the end of the body, excluding the hind legs. The terminology used to describe oral cavity armature and egg shell morphology follows Michalczyk & Kaczmarek (2003) and Kaczmarek & Michalczyk (2017a). The type of buccal apparatus and claws are given according to Pilato & Binda (2010). Macroplacoid length sequence is given according to Kaczmarek *et al.* (2014b). Buccal tube length and the level of the stylet support insertion point were measured according to Pilato (1981). The *pt* index is the ratio of the length of a given structure to the length of the buccal tube expressed as a percentage (Pilato 1981). All other measurements and nomenclature follow Kaczmarek & Michalczyk (2017a). Morphometric data were handled using the 'Parachela' ver. 1.6 template available from the Tardigrada Register (Michalczyk & Kaczmarek 2013). Raw morphometric data for each analysed species are provided as supplementary materials (SM.01 and SM.02) Tardigrade taxonomy follows Guil *et al.* (2019).

### Genotyping

The DNA was extracted from individual animals following a Chelex® 100 resin (Bio-Rad) extraction method by Casquet *et al.* (2012) with modifications described in detail in Stec *et al.* (2015). Before the extraction, live specimens were mounted in water slides and checked under the microscope to confirm their identification. We sequenced four DNA fragments: the small ribosome subunit (18S rRNA, nDNA), the large ribosome subunit (28S rRNA, nDNA), the internal transcribed spacer (ITS-2, nDNA) and the cytochrome oxidase subunit I (COI, mtDNA). All fragments were amplified and sequenced according to the protocols described in Stec *et al.* (2015); primers and original references for specific PCR programs are listed in Table 1. Sequencing products were read with the ABI 3130xl sequencer at the Molecular Ecology Lab, Institute of Environmental Sciences of the Jagiellonian University, Kraków, Poland. Sequences were processed in BioEdit ver. 7.2.5 (Hall 1999) and submitted to GenBank.

### Comparative molecular and phylogenetic analysis

For molecular comparisons, all published sequences of the four above-mentioned markers for species of the *hufelandi* complex were downloaded from GenBank (Appendix 1). The sequences were aligned using the default settings (in the case of ITS-2 and COI) and the Q-INS-I method (in the case of ribosomal markers: 18S rRNA, 28S rRNA) of MAFFT ver. 7 (Katoh *et al.* 2002; Katoh & Toh 2008) and manually checked against non-conservative alignments in BioEdit. Then, the aligned sequences were trimmed to 763 (18S rRNA), 715 (28S rRNA), 352 (ITS-2) and 618 (COI) bp. All COI sequences were translated into protein sequences in MEGA7 ver. 7.0 (Kumar *et al.* 2016) to check against pseudogenes. Uncorrected pairwise distances were calculated using MEGA7 and are provided as supplementary materials (SM.03).

**Table 1.** Primers and references for PCR protocols for amplification of the four DNA fragments sequenced in the study.

| DNA fragment | Primer name | Primer direction | Primer sequence (5′-3′) | Primer source | PCR programme |
|---|---|---|---|---|---|
| **18S rRNA** | 18S_Tar_1Ff | forward | AGGCGAAACCGCGAATGGCTC | Stec *et al.* (2017a) | Zeller (2010) |
| | 18S_Tar_1Rr | reverse | GCCGCAGGCTCCACTCCTGG | | |
| **28S rRNA** | 28S_Eutar_F | forward | ACCCGCTGAACTTAAGCATAT | Gąsiorek *et al.* (2018); Mironov *et al.* (2012) | Mironov *et al.* (2012) |
| | 28SR0990 | reverse | CCTTGGTCCGTGTTTCAAGAC | | |
| **ITS-2** | Eutar_Ff | forward | CGTAACGTGAATTGCAGGAC | Stec *et al.* (2018c) | Stec *et al.* (2018c) |
| | Eutar_Rr | reverse | TCCTCCGCTTATTGATATGC | | |
| **COI** | LCO1490 | forward | GGTCAACAAATCATAAAGATATTGG | Folmer *et al.* (1994) | Michalczyk *et al.* (2012) |
| | HCO2198 | reverse | TAAACTTCAGGGTGACCAAAAAATCA | | |

In order to verify the phylogenetic position of the new species, a phylogenetic tree was constructed on published COI sequences of species from the *M. hufelandi* complex (see Appendix 1 for all references) with four species of *Mesobiotus* Vecchi, Cesari, Bertolani, Jönsson, Rebecchi & Guidetti, 2016 as the outgroup. Specifically, these were: *Mesobiotus hilariae* (accession number: KT226108) described by Vecchi *et al.* (2016), *Mesobiotus philippinicus* (accession number: KX129796) described by Mapalo *et al.* 2016, *Mesobiotus insanis* (accession number: MF441491) described by Mapalo *et al.* 2017 and *Mesobiotus ethiopicus* (accession number: MF678794) described by Stec & Kristensen (2017). Since the COI is a protein coding gene, before partitioning, we divided our alignment into 3 data blocks constituting the three separate codon positions using PartitionFinder ver. 2.1.1 (Lanfear *et al.* 2016) under the Bayesian Information Criterion (BIC). The best scheme of partitioning and substitution models were chosen for posterior phylogenetic analysis. We ran the analysis to test all possible models implemented in the program. As best-fit partitioning scheme, PartitionFinder suggested to retain three predefined partitions separately. The best-fit models for these partitions were: SYM+I+G for the first codon position, GTR+I+G for the second codon position and HKY+G for the third codon position. Bayesian inference (BI) marginal posterior probabilities were calculated using MrBayes ver. 3.2 (Ronquist & Huelsenbeck 2003). Random starting trees were used and the analysis was run for eight million generations, sampling the Markov chain every 1000 generations. An average standard deviation of split frequencies of < 0.01 was used as a guide to ensure the two independent analyses had converged. The program Tracer ver. 1.3 (Rambaut *et al.* 2018) was then used to ensure Markov chains had reached stationarity and to determine the correct 'burn-in' for the analysis, which was the first 10% of generations. A consensus tree was obtained after summarising the resulting topologies and discarding the 'burn-in'. All final consensus tree were viewed and visualised by FigTree ver. 1.4.3 (available from http://tree.bio.ed.ac.uk/software/figtree).

**Abbreviations**

IZiBB = Institute of Zoology and Biomedical Research, Jagiellonian University, Gronostajowa 9, 30-387, Kraków, Poland
PCM = Phase Contrast light Microscopy
SEM = Scanning Electron Microscopy

## Results

### *Taxonomic account of the new species*

Phylum Tardigrada Doyère, 1840
Class Eutardigrada Richters, 1926
Order Macrobiotoidea Guil *et al.*, 2019
Family Macrobiotidae Thulin, 1928
Genus *Macrobiotus* Schultze, 1834

***Macrobiotus noongaris*** sp. nov.
urn:lsid:zoobank.org:act:A7BF7FF6-451F-4382-A842-CAC1EF51E6B8
Figs 1–7

#### Etymology

The name refers to the indigenous Australians who live in the region where the new species was found. These are the Noongar peoples, 14 different but related language groups that occupied these lands before western settlement, including the modern city of Perth where the sample was collected. In their languages, the term Noongar means 'a person of the southwest of Western Australia'.

#### Material examined

86 animals (including 31 simplex) and 57 eggs. Specimens mounted on microscope slides in Hoyer's medium (72 animals + 47 eggs), fixed on SEM stubs (10+10) and processed for DNA sequencing (4+0).

**Holotype**
AUSTRALIA – **Western Australia** • ♀; Perth, Kings Park; 31°57′30″ S, 115°350′09″ E; 46 m a.s.l.; moss on soil in an urban park; IZiBB AU.031.12.

**Paratypes**
AUSTRALIA – **Western Australia** • 62 paratypes; same collection data as for holotype; IZiBB AU.031.06 to AU.031.14 • 32 eggs; same collection data as for holotype; IZiBB AU.031.02–05.

#### Description

**Animals** (measurements and statistics in Table 2)
Body transparent in juveniles and white in adults but transparent after fixation in Hoyer's medium (Fig. 1A). Eyes present in live animals as well as in specimens mounted in Hoyer's medium. Small round and oval cuticular pores (0.3–0.8 µm in diameter), visible under both PCM and SEM, scattered randomly on entire body (Fig. 1B–C). Granulation present on all legs (Fig. 2A–F). A patch of clearly visible granulation present on external surface of legs I–III (Fig. 2A–B). A cuticular bulge/fold (pulvinus) present on internal surface of legs I–III, with a faint cuticular fold covered with faint granulation and paired muscles attachments just above the claws (Fig. 2C–D). Both structures are visible only if legs are fully extended and properly oriented on slide (particularly in the case of the pulvinus and cuticular fold). Granulation on legs IV always clearly visible and consists of a single large granulation patch on each leg (Fig. 2E–F).

Claws stout, of *hufelandi* type (Fig. 3A–D). Primary branches with distinct accessory points, a common tract, and with an evident stalk connecting claw to lunula (Fig. 3A–D). Lunulae I–III smooth (Fig. 3A, C), whereas lunulae IV clearly dentate (Fig. 3B, D). Cuticular bars under claws absent. Double muscle attachments faintly marked under PCM but clearly visible under SEM (Fig. 3A, C).

**Table 2.** Measurements (in µm) and *pt* values of selected morphological structures of the holotype and paratypes of *Macrobiotus noongaris* sp. nov. mounted in Hoyer's medium (N = number of specimens/structures measured; Range = the smallest and the largest structure among all measured specimens; SD = standard deviation).

| Character | N | Range | | Mean | | SD | | Holotype | |
|---|---|---|---|---|---|---|---|---|---|
| | | µm | *pt* | µm | *pt* | µm | *pt* | µm | *pt* |
| Body length | 30 | 333–557 | *1039–1332* | 461 | *1201* | 56 | *71* | 443 | *1205* |
| Buccopharyngeal tube | | | | | | | | | |
| Buccal tube length | 30 | 31.8–43.5 | | 38.3 | – | 3.4 | – | 36.8 | – |
| Stylet support insertion point | 30 | 24.7–34.6 | *76.7–81.6* | 30.2 | *78.7* | 2.8 | *1.0* | 28.8 | *78.3* |
| Buccal tube external width | 30 | 4.4–7.4 | *13.8–17.9* | 5.9 | *15.5* | 0.7 | *1.0* | 5.7 | *15.4* |
| Buccal tube internal width | 30 | 2.9–5.0 | *8.0–11.9* | 4.1 | *10.6* | 0.6 | *0.9* | 3.7 | *10.1* |
| Ventral lamina length | 30 | 19.4–27.8 | *55.4–70.2* | 23.4 | *61.1* | 2.1 | *3.2* | 22.0 | *59.7* |
| Placoid lengths | | | | | | | | | |
| Macroplacoid 1 | 30 | 8.0–12.7 | *24.5–3.6* | 10.6 | *27.6* | 1.4 | *1.7* | 10.5 | *28.5* |
| Macroplacoid 2 | 30 | 5.2–8.8 | *15.0–21.0* | 7.0 | *18.3* | 1.1 | *1.6* | 6.1 | *16.5* |
| Microplacoid | 30 | 2.0–4.2 | *6.2–9.7* | 3.1 | *8.0* | 0.5 | *1.0* | 2.9 | *7.9* |
| Macroplacoid row | 30 | 13.9–22.7 | *41.9–57.7* | 18.4 | *47.9* | 2.6 | *3.5* | 17.1 | *46.5* |
| Placoid row | 30 | 16.4–26.1 | *51.3–63.7* | 22.1 | *57.5* | 2.8 | *3.3* | 21.2 | *57.6* |
| Claw 1 heights | | | | | | | | | |
| External primary branch | 30 | 7.5–10.9 | *20.8–28.7* | 9.6 | *25.2* | 0.9 | *2.1* | 10.4 | *28.3* |
| External secondary branch | 30 | 5.5–9.4 | *14.8–24.3* | 7.5 | *19.6* | 1.1 | *2.5* | 8.4 | *22.9* |
| Internal primary branch | 30 | 6.7–10.2 | *19.2–29.6* | 9.0 | *23.7* | 0.8 | *2.3* | 9.2 | *24.9* |
| Internal secondary branch | 30 | 5.4–8.2 | *16.6–22.1* | 7.3 | *19.1* | 0.7 | *1.7* | 7.8 | *21.1* |
| Claw 2 heights | | | | | | | | | |
| External primary branch | 30 | 8.5–12.1 | *22.9–32.9* | 10.5 | *27.6* | 0.8 | *2.5* | 12.1 | *32.9* |
| External secondary branch | 30 | 6.1–9.9 | *16.6–26.5* | 8.4 | *22.0* | 0.9 | *2.3* | 9.1 | *24.7* |
| Internal primary branch | 30 | 7.9–10.3 | *20.9–29.3* | 9.5 | *24.9* | 0.6 | *1.9* | 9.4 | *25.6* |
| Internal secondary branch | 30 | 6.5–8.8 | *16.4–24.9* | 7.7 | *20.3* | 0.7 | *2.0* | 8.8 | *23.9* |
| Claw 3 heights | | | | | | | | | |
| External primary branch | 30 | 8.8–11.9 | *23.6–32.7* | 10.5 | *27.4* | 0.7 | *2.1* | 11.3 | *30.6* |
| External secondary branch | 30 | 6.1–9.7 | *17.9–25.8* | 8.3 | *21.8* | 0.8 | *2.1* | 8.9 | *24.2* |
| Internal primary branch | 30 | 7.4–10.7 | *22.4–29.6* | 9.5 | *24.8* | 0.7 | *1.8* | 9.5 | *25.8* |
| Internal secondary branch | 30 | 5.5–9.3 | *16.6–25.2* | 7.5 | *19.6* | 0.9 | *2.0* | 9.3 | *25.2* |
| Claw 4 lengths | | | | | | | | | |
| Anterior primary branch | 30 | 8.2–12.3 | *22.7–32.2* | 10.5 | *27.5* | 1.1 | *2.6* | 11.8 | *32.2* |
| Anterior secondary branch | 30 | 5.4–9.7 | *15.7–25.1* | 8.0 | *21.0* | 1.0 | *2.4* | 9.2 | *25.1* |
| Posterior primary branch | 30 | 8.6–12.0 | *23.1–32.7* | 10.5 | *27.5* | 0.8 | *2.6* | 11.1 | *30.3* |
| Posterior secondary branch | 30 | 5.6–9.5 | *16.3–26.5* | 8.0 | *21.0* | 1.1 | *2.6* | 8.9 | *24.1* |

Mouth antero-ventral followed by ten peribuccal lamellae and a circular sensory lobe (Figs 4A, 5A). Bucco-pharyngeal apparatus of *Macrobiotus* type (Fig. 4A). Under PCM, oral cavity armature of the *patagonicus* type, i.e., with only 2nd and 3rd bands of teeth visible (Fig. 4B–C). However, in SEM all three bands of teeth visible, with first band being situated at base of peribuccal lamellae and composed of a single row of small fused cone-shaped teeth connected to form a continuous, slightly serrated ring ridge around oral cavity (Fig. 5B–C). Second band of teeth situated between ring fold and third band of teeth and comprises 3–6 rows of small cone-shaped teeth (Figs 4B–C, 5B–C). Teeth of third band located within posterior portion of oral cavity, between second band of teeth and buccal tube opening (Figs 4B–C, 5B–C). Third band of teeth discontinuous and divided into dorsal and ventral portions. Under PCM, dorsal teeth appear as three distinct transverse ridges, whereas ventral teeth appear as

two separate lateral transverse ridges and a median tooth (Fig. 4B–C). In SEM, both dorsal and ventral teeth also clearly distinct (Fig. 5B–C). Under SEM, margins of medio-dorsal tooth slightly serrated (Fig. 5B), whereas the medio-ventral tooth slightly anterior to lateral teeth (Fig. 5C). Pharyngeal bulb spherical, with triangular apophyses, two rod-shaped macroplacoids and a small triangular microplacoid (Fig. 4A, D–E). Macroplacoid length sequence 2 < 1. First macroplacoid exhibits central constriction, whereas second macroplacoid sub-terminally constricted (Fig. 4A, D–E).

**Eggs** (measurements and statistics in Table 3)
Laid freely, white, spherical or slightly ovoid (Fig. 6A). Surface between processes is of the *hufelandi* type, i.e., covered with a reticulum (Figs 6E, 7B–D, F). Meshes of reticulum small (0.1–0.6 µm) and rounded, regular in size and with blurred rims in PCM (Fig. 6E), irregular in size and with thick borders in SEM (meshes in SEM appear as pores; Figs 7B–D, F). Interbasal meshes larger than peribasal meshes, but peribasal meshes do not form rings around process bases (Figs 6E, 7B–D, F). Eggs have 22–30 processes on circumference, 26 on average (Fig. 6A). Processes are of inverted goblet shape, with slightly concave trunks and concave terminal discs (Figs 6C–E, 7B–E). Terminal discs are round

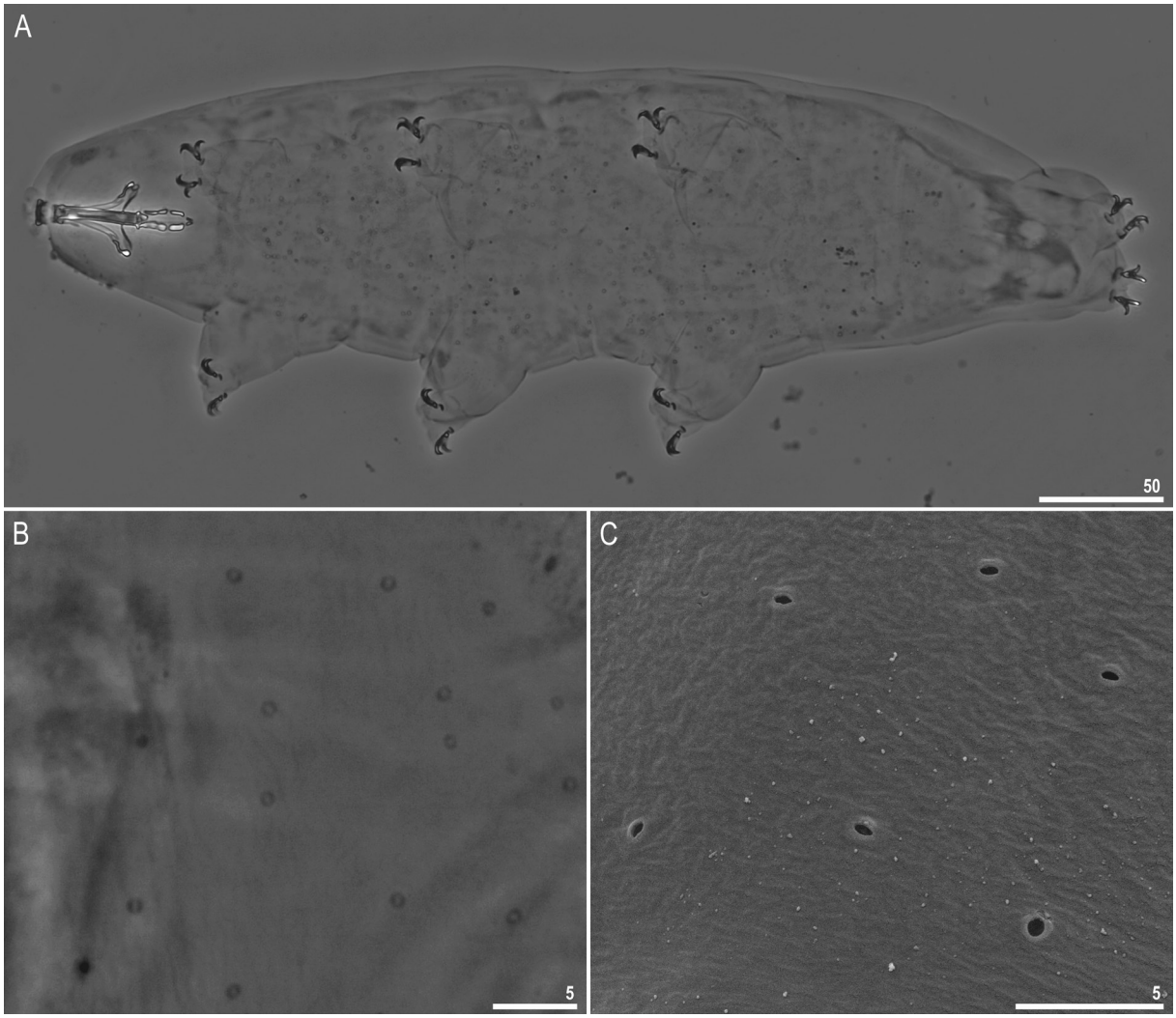


**Fig. 1.** *Macrobiotus noongaris* sp. nov., habitus. **A**. Dorso-ventral projection (holotype, Hoyer's medium, PCM, IZiBB AU.031.12). **B–C**. Cuticular pores on the dorsal part of the body seen in PCM (B: holotype) and in SEM (C: paratype, IZiBB). Scale bars in µm.

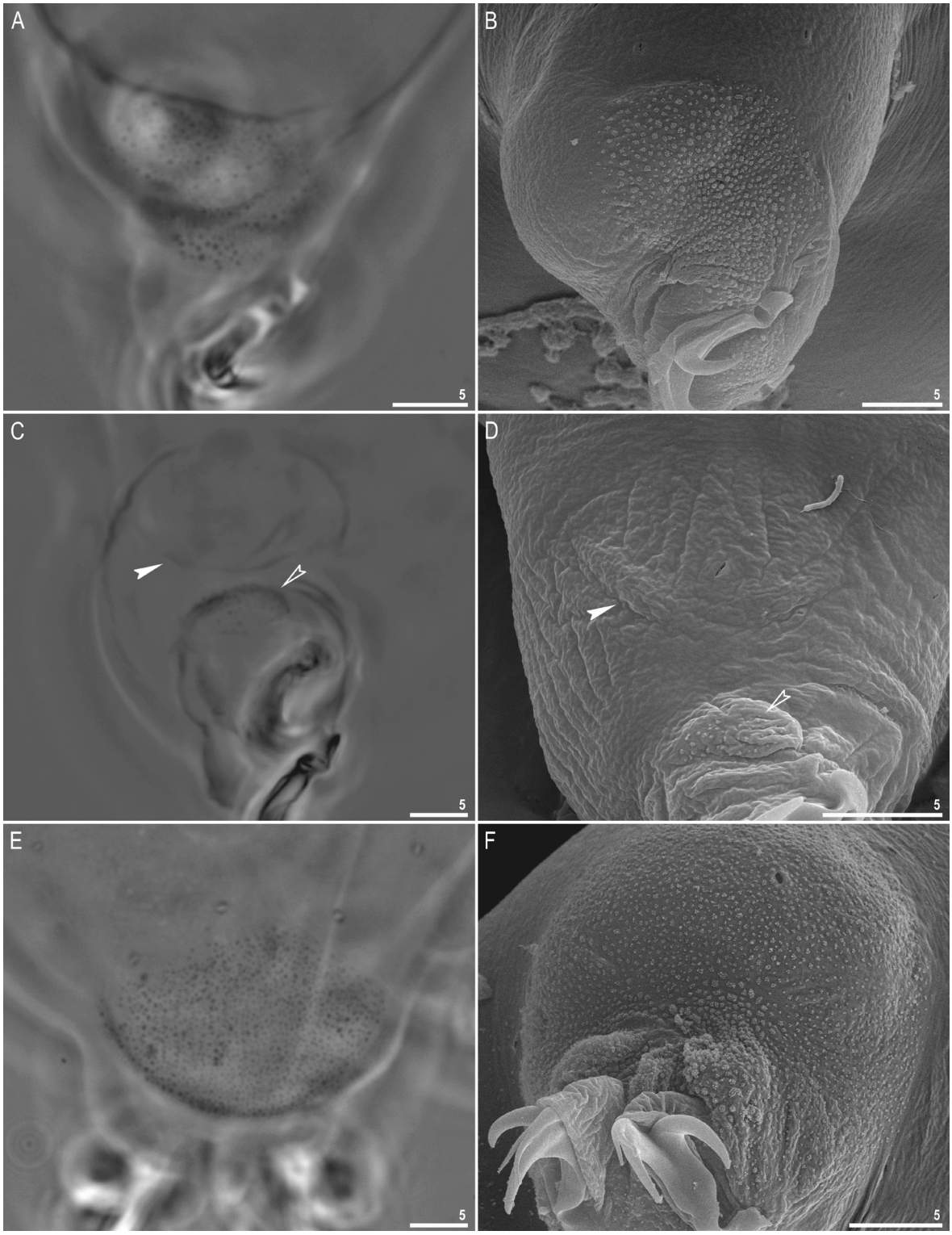


**Fig. 2.** *Macrobiotus noongaris* sp. nov., cuticular structures on legs (paratypes, IZiBB). **A–B**. External granulation on legs II and III seen in PCM (A) and SEM (B), respectively. **C–D**. A cuticular bulge (pulvinus) and a faint cuticular fold, covered by granulation, on the internal surface of legs I and III seen in PCM (C) and SEM (D), respectively. **E–F**. Granulation on leg IV seen in PCM (E) and SEM (F). Filled indented arrowheads indicate the cuticular bulge and empty indented arrowheads indicate the faint cuticular fold under the claws. Scale bars in μm.

**Table 3.** Measurements (in μm) of selected morphological structures of the eggs of *Macrobiotus noongaris* sp. nov. mounted in Hoyer's medium (N = number of eggs/structures measured; Range = the smallest and the largest structure among all measured specimens; SD = standard deviation).

| Character | N | Range | Mean | SD |
|---|---|---|---|---|
| Egg bare diameter | 30 | 62.5–81.7 | 70.7 | 5.0 |
| Egg full diameter | 30 | 73.2–92.5 | 82.1 | 5.5 |
| Process height | 90 | 4.5–8.4 | 6.2 | 0.7 |
| Process base width | 90 | 3.4–6.6 | 5.0 | 0.7 |
| Process base/height ratio | 90 | 56%–128% | 81% | 12% |
| Terminal disc width | 90 | 2.3–4.8 | 3.3 | 0.5 |
| Inter-process distance | 90 | 2.2–5.1 | 3.4 | 0.5 |
| Number of processes on egg circumference | 30 | 22–30 | 26.1 | 1.7 |

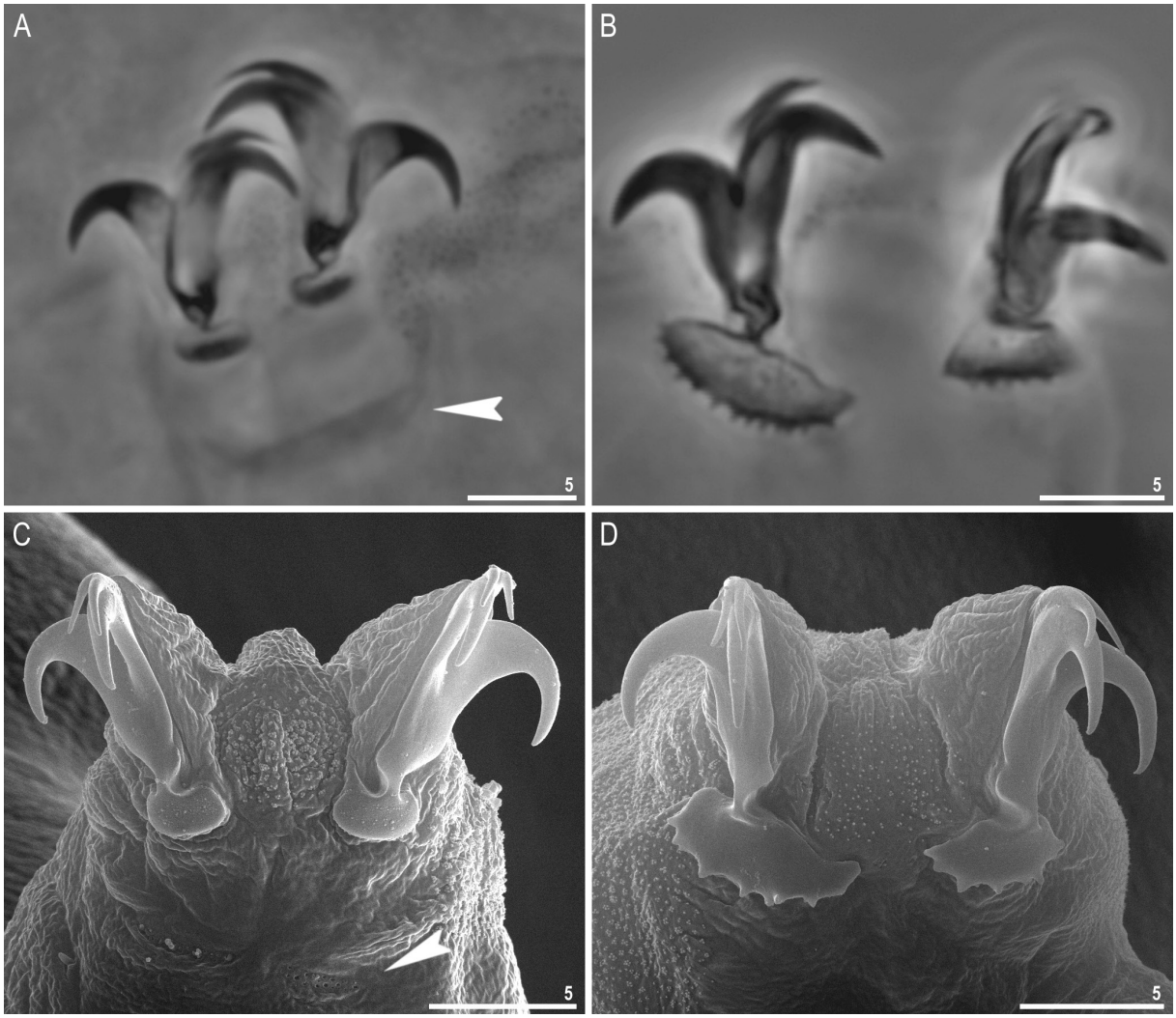


**Fig. 3.** *Macrobiotus noongaris* sp. nov., claws (paratypes, IZiBB). **A–B**. Claws II and IV seen in PCM, with smooth and dentate lunules, respectively. **C–D**. Claws I and IV seen in SEM, with smooth and dentate lunules, respectively. Filled indented arrowheads indicate double muscle attachments under the claws. Scale bars in μm.

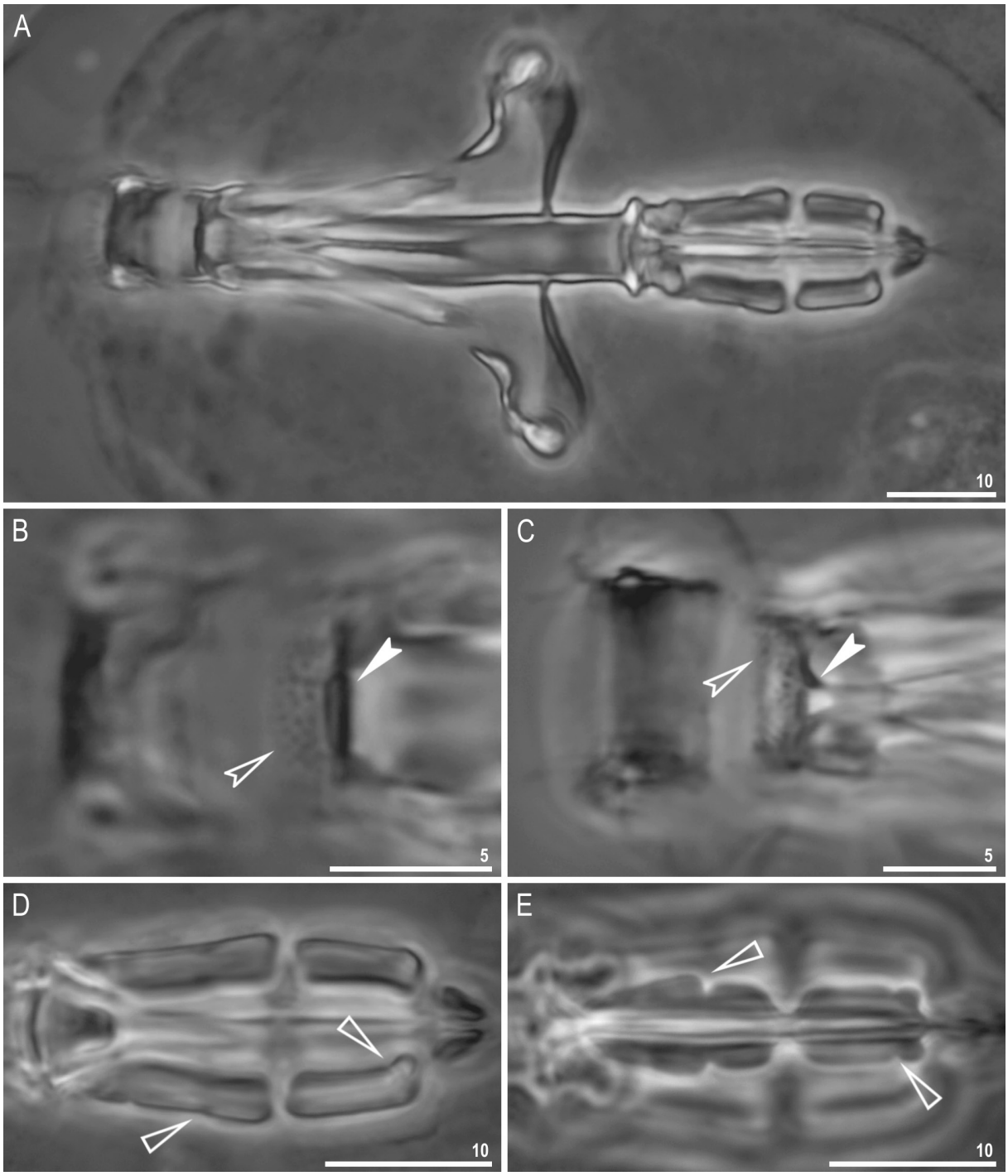


**Fig. 4.** *Macrobiotus noongaris* sp. nov., buccal apparatus and the oral cavity armature seen in PCM (paratypes, IZiBB). **A**. Dorso-ventral projection of the entire buccal apparatus. **B–C**. Oral cavity armature visible in dorsal (B) and ventral (C) views, respectively. **D–E**. Placoid morphology visible in dorsal (D) and ventral (E) views, respectively. Empty indented arrowheads indicate the second band of teeth in the oral cavity, filled indented arrowheads indicate the third band of teeth in the oral cavity, empty flat arrowheads indicate central constrictions in first macroplacoids and subterminal constriction in second macroplacoids. Scale bars in μm.

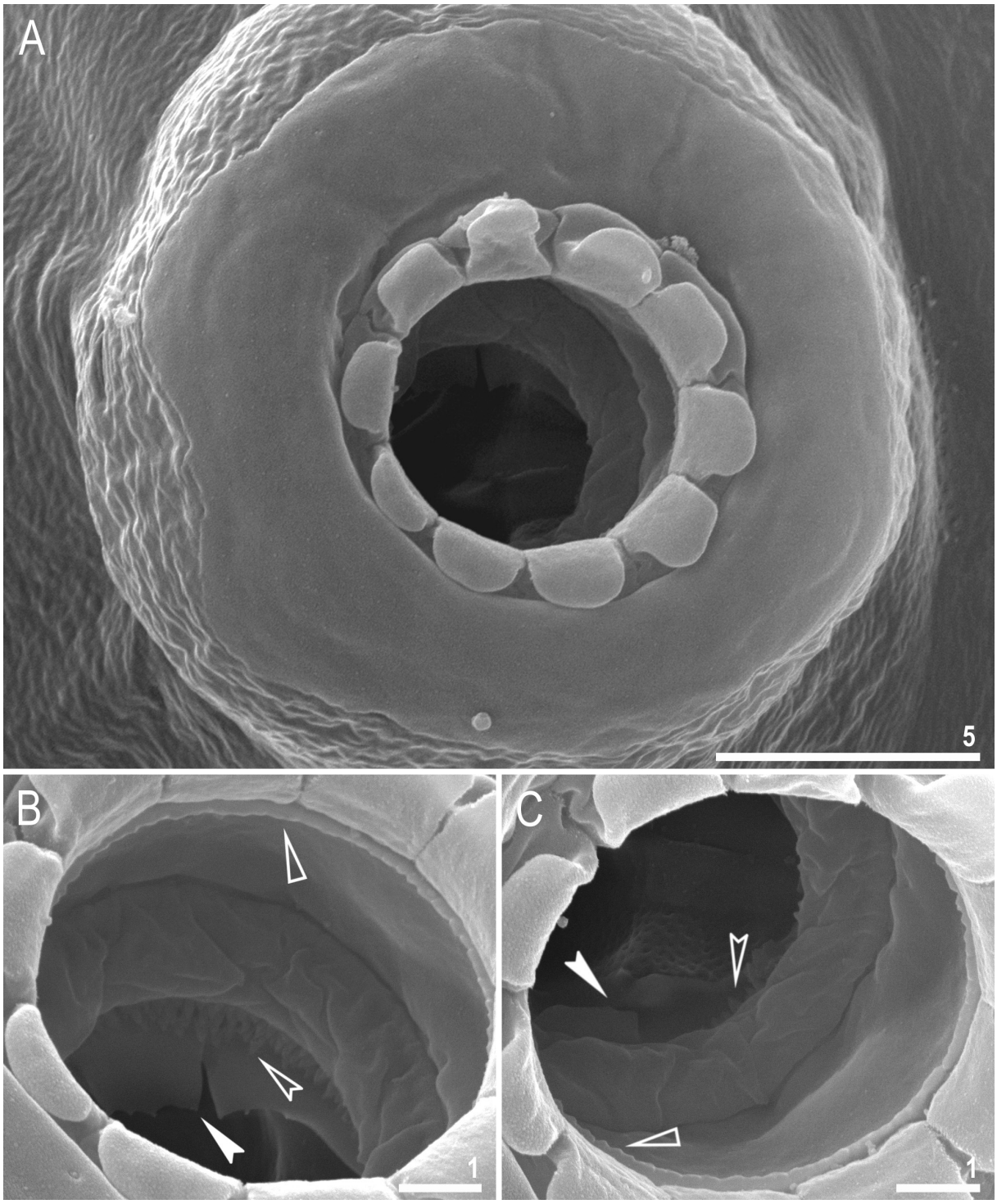


**Fig. 5.** *Macrobiotus noongaris* sp. nov., mouth opening and the oral cavity armature seen in SEM (paratype, IZiBB). **A**. Mouth opening with peribuccal sensory lobes and ten peribuccal lamellae. **B–C**. The oral cavity armature of a single paratype seen in SEM from different angles, in dorsal (B) and ventral (C) views, respectively. Empty flat arrowheads indicate the first band of teeth in the oral cavity, empty indented arrowheads indicate the second band of teeth in the oral cavity, filled indented arrowheads indicate the third band of teeth in the oral cavity. Scale bars in μm.

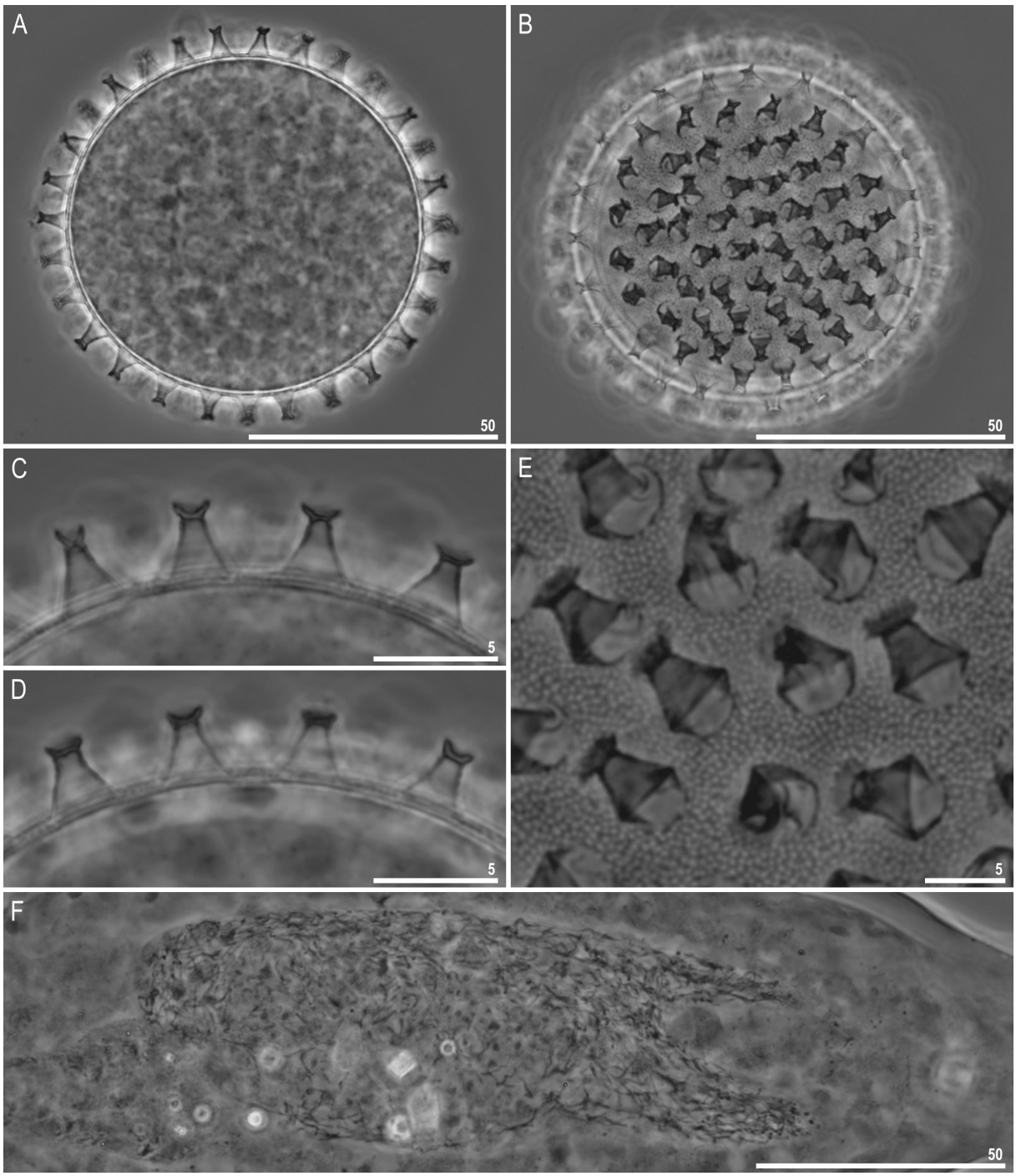


**Fig. 6.** *Macrobiotus noongaris* sp. nov. **A–E**. Egg, seen in PCM (IZiBB). **A**. Midsection under 400× magnification. **B**. Surface under 400× magnification. **C–D**. Midsection under 1000× magnification. **E**. Surface and terminal discs under 1000× magnification. **F**. Testis seen in PCM, with visible spermatozoa in male freshly mounted in Hoyer's medium (paratype, IZiBB). Scale bars in μm.

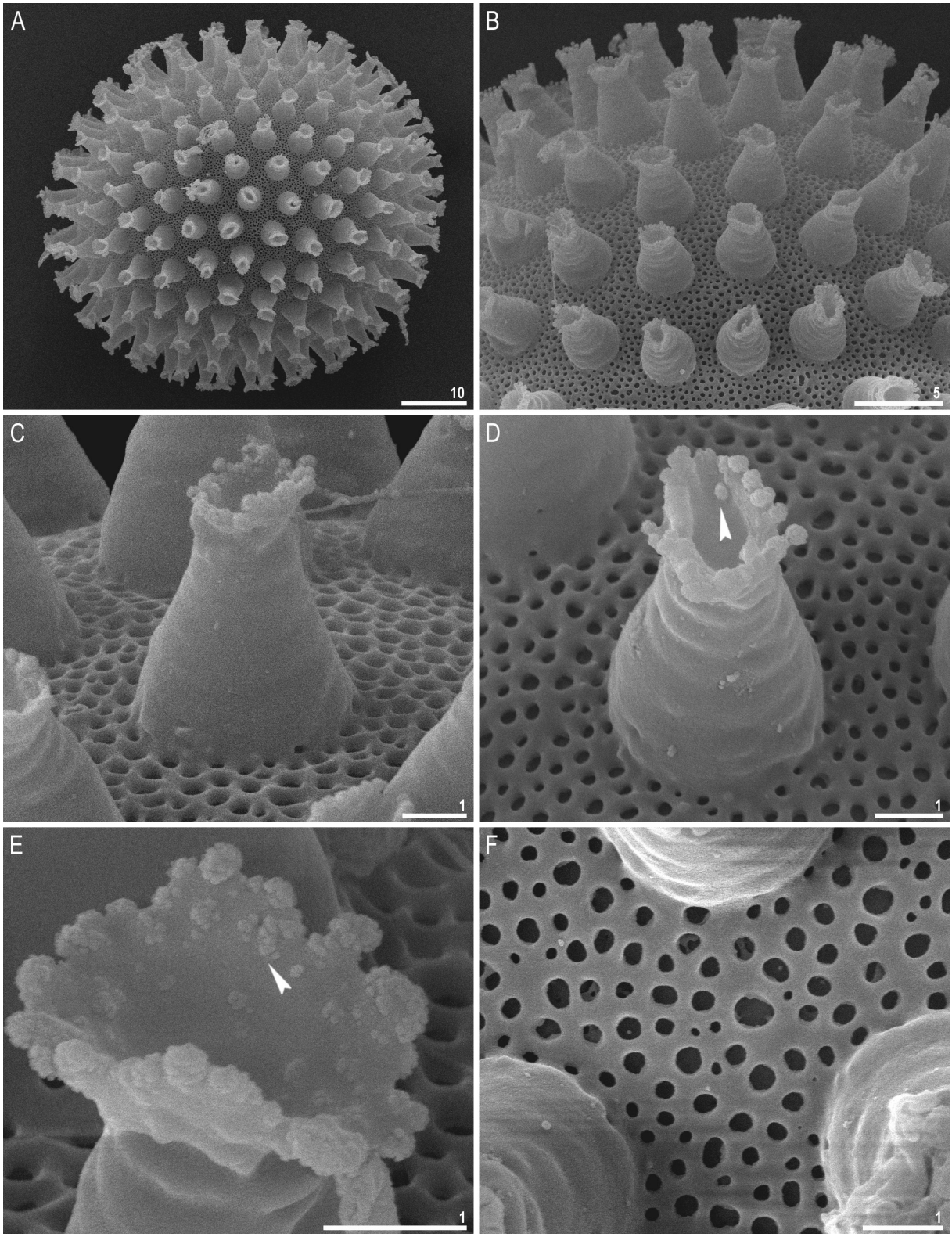


**Fig. 7.** *Macrobiotus noongaris* sp. nov., egg chorion morphology seen in SEM (IZiBB). **A**. Entire egg. **B**. Magnification of the egg surface. **C–D**. Details of the egg processes. **E**. Terminal disc. **F**. Details of the reticulation between egg processes. Arrowheads indicate scattered granulation on the terminal disc surface. Scale bars in μm.

and strongly serrated (Fig. 7C–E). Each terminal disc has a distinct concave central area which may contain some scattered granulation within, which is also always present on the margin (visible only under SEM; Fig. 7C–E).

**Reproduction**

The new species is dioecious. No spermathecae filled with sperm have been found in gravid females on the freshly prepared slides. However, the testis in males, filled with spermatozoa, is clearly visible under PCM up to 24 hours after mounting in Hoyer's medium (Fig. 6F). The new species does not exhibit male secondary sexual dimorphism traits such as lateral gibbosities on legs IV.

**DNA sequences**

We obtained sequences for all four of the above mentioned DNA markers. All sequenced fragments were represented by single haplotypes except the ITS-2, in which two distinct haplotypes were present:

The 18S rRNA sequence (GenBank: MK737069), 1010 bp long.
The 28S rRNA sequence (GenBank: MK737063), 786 bp long.
The ITS-2 haplotype 1 sequence (GenBank: MK737065), 418 bp long.
The ITS-2 haplotype 2 sequence (GenBank: MK737066), 418 bp long.
The COI sequence (GenBank: MK737919), 658 bp long.

***Macrobiotus kamilae*** sp. nov.
urn:lsid:zoobank.org:act:AA314AF2-9A60-47E3-9EB3-B8B249FC1580
Figs 8–15

**Etymology**

We take great pleasure in dedicating this new species to the friend of the second author, Kamila Zając, who is a young malacologist and a PhD student at the Institute of Environmental Sciences, Jagiellonian University, Kraków, Poland.

**Material examined**

77 animals (including 19 simplex) and 42 eggs. Specimens mounted on microscope slides in Hoyer's medium (63 animals + 32 eggs), fixed on SEM stubs (10+10) and processed for DNA sequencing (4+0).

**Holotype**

INDIA – **Chuy Province** • ♀; Camel's Back Road, Mussoorie, Dehradin District, Uttarakhand State; 30°27′28″ N, 78°04′41″ E; 2001 m a.s.l.; moss on rock; IZiBB IN.030.08.

**Paratypes**

INDIA – **Chuy Province** • 71 paratypes; same collection data as for holotype; IZiBB IN.030.01–06, IN.030.08–12, IN.030.14–15, IN.030.18–19 • 47 eggs; same collection data as for holotype; IZiBB IN.030.13, IN.030.16–17, IN.030.20.

**Description**

**Animals** (measurements and statistics in Table 4)

Body transparent in juveniles and yellowish in adults, but transparent after fixation in Hoyer's medium (Fig. 8A). Eyes present in live animals as well as in specimens mounted in Hoyer's medium. Small round and oval cuticular pores (0.3–0.8 μm in diameter), visible under both PCM and SEM, scattered randomly on entire body (Fig. 8B–C). Granulation present on all legs (Fig. 9A–F). A patch of clearly visible granulation present on external surface of legs I–III (Fig. 9A–B). A cuticular bulge/fold (pulvinus)

**Table 4.** Measurements (in µm) and *pt* values of selected morphological structures of the holotype and paratypes of *Macrobiotus kamilae* sp. nov. mounted in Hoyer's medium (N = number of specimens / structures measured; Range = the smallest and the largest structure among all measured specimens; SD = standard deviation).

| Character | N | Range | | Mean | | SD | | Holotype | |
|---|---|---|---|---|---|---|---|---|---|
| | | µm | *pt* | µm | *pt* | µm | *pt* | µm | *pt* |
| Body length | 30 | 367–569 | *1019–1430* | 477 | *1232* | 59 | *107* | 569 | *1292* |
| Buccopharyngeal tube | | | | | | | | | |
| Buccal tube length | 30 | 33.1–44.0 | – | 38.7 | – | 2.7 | – | 44.0 | – |
| Stylet support insertion point | 30 | 23.7–32.1 | *71.6–75.9* | 28.5 | *73.6* | 2.1 | *1.1* | 32.1 | *72.9* |
| Buccal tube external width | 30 | 4.1–6.0 | *10.6–15.6* | 5.1 | *13.1* | 0.5 | *1.0* | 5.5 | *12.5* |
| Buccal tube internal width | 30 | 2.4–4.3 | *6.1–10.3* | 3.4 | *8.9* | 0.5 | *0.9* | 4.0 | *9.0* |
| Ventral lamina length | 30 | 18.1–29.2 | *50.5–68.4* | 22.8 | *58.8* | 2.5 | *3.7* | 27.1 | *61.5* |
| Placoid lengths | | | | | | | | | |
| Macroplacoid 1 | 30 | 8.1–13.7 | *23.0–35.3* | 10.6 | *27.4* | 1.6 | *3.1* | 13.7 | *31.1* |
| Macroplacoid 2 | 30 | 4.8–8.0 | *13.5–19.1* | 6.4 | *16.6* | 0.9 | *1.5* | 8.0 | *18.1* |
| Microplacoid | 30 | 2.4–4.0 | *6.3–9.7* | 3.2 | *8.2* | 0.5 | *1.0* | 2.9 | *6.6* |
| Macroplacoid row | 30 | 14.2–22.3 | *39.1–56.1* | 18.1 | *46.8* | 2.4 | *4.4* | 22.3 | *50.7* |
| Placoid row | 30 | 17.1–26.7 | *48.1–66.4* | 21.9 | *56.7* | 2.6 | *4.5* | 25.6 | *58.2* |
| Claw 1 heights | | | | | | | | | |
| External primary branch | 30 | 10.4–16.9 | *26.7–41.2* | 13.9 | *35.9* | 1.5 | *2.7* | 16.8 | *38.0* |
| External secondary branch | 30 | 6.8–12.9 | *18.3–31.7* | 10.4 | *27.0* | 1.3 | *3.1* | 12.9 | *29.2* |
| Internal primary branch | 30 | 10.1–16.6 | *28.5–41.1* | 12.9 | *33.4* | 1.6 | *2.8* | 15.9 | *36.1* |
| Internal secondary branch | 30 | 7.5–12.8 | *20.1–31.6* | 10.0 | *26.0* | 1.3 | *2.7* | 12.0 | *27.2* |
| Claw 2 heights | | | | | | | | | |
| External primary branch | 30 | 10.3–19.2 | *26.5–46.6* | 15.0 | *38.8* | 2.0 | *3.8* | 19.1 | *43.3* |
| External secondary branch | 30 | 7.5–15.4 | *19.8–34.9* | 11.3 | *29.2* | 1.8 | *3.7* | 15.4 | *34.9* |
| Internal primary branch | 30 | 9.3–17.1 | *23.7–41.1* | 13.5 | *34.8* | 1.7 | *3.2* | 17.1 | *38.9* |
| Internal secondary branch | 30 | 8.1–12.8 | *20.7–32.1* | 10.5 | *27.1* | 1.3 | *3.0* | 12.8 | *29.1* |
| Claw 3 heights | | | | | | | | | |
| External primary branch | 30 | 12.1–18.8 | *32.1–44.4* | 14.9 | *38.4* | 1.6 | *2.7* | 18.8 | *42.7* |
| External secondary branch | 30 | 7.4–14.6 | *18.2–34.5* | 11.2 | *29.1* | 1.6 | *3.9* | 14.6 | *33.0* |
| Internal primary branch | 30 | 9.9–17.6 | *27.3–41.8* | 13.4 | *34.6* | 1.7 | *2.9* | 17.0 | *38.6* |
| Internal secondary branch | 30 | 8.0–13.7 | *21.5–33.5* | 10.7 | *27.7* | 1.4 | *2.8* | 13.4 | *30.5* |
| Claw 4 lengths | | | | | | | | | |
| Anterior primary branch | 30 | 12.5–20.2 | *32.0–46.8* | 15.8 | *40.8* | 1.8 | *3.5* | 20.2 | *45.8* |
| Anterior secondary branch | 30 | 7.7–14.5 | *18.7–34.9* | 11.8 | *30.5* | 1.4 | *3.2* | 14.0 | *31.7* |
| Posterior primary branch | 30 | 13.5–19.8 | *34.4–48.3* | 16.2 | *41.8* | 1.7 | *3.3* | 19.7 | *44.8* |
| Posterior secondary branch | 30 | 7.6–14.2 | *19.4–34.7* | 11.4 | *29.5* | 1.2 | *2.8* | 12.6 | *28.5* |

present on internal surface of legs I–III, with a faint cuticular fold and a patch of granulation between them (Fig. 9C–D). Both structures visible only if legs fully extended and properly oriented on slide. Cuticular granulation on legs IV always clearly visible and consisting of a single large granulation patch on each leg (Fig. 9E–F). In addition to granulation on legs, three patches of granulation on body located dorso-laterally between legs III and IV, with granule size and density increasing from 1st to 3rd patch (Fig. 10A–E).

Claws long and slender, of the *hufelandi* type (Fig. 11A–D). Primary branches with distinct accessory points, a long common tract and with an evident stalk connecting the claw to the lunula (Fig. 11A–D). Lunulae I–III smooth (Fig. 11A, C), whereas lunulae IV clearly dentate (Fig. 11B, D). Cuticular bars under claws are absent. Double muscle attachments are faintly marked under PCM but clearly visible under SEM (Fig. 11A, C, respectively). A faintly marked horseshoe structure connecting the anterior and the posterior claw is visible only in PCM (Fig. 11B, D).

Mouth antero-ventral with ten peribuccal lamellae and a circular sensory lobe (Figs 12A, 13A). Buccopharyngeal apparatus of the *Macrobiotus* type (Fig. 12A). Under PCM, the oral cavity armature is of the *patagonicus* type, i.e., with only the 2nd and 3rd bands of teeth visible (Fig. 12B–E). However, in SEM all three bands of teeth are visible, with the first band being situated at the base of peribuccal lamellae and composed of a single row of small cone-shaped teeth. The second band of teeth is situated between the ring fold and the third band of teeth and comprises 2–4 rows of small cone-shaped teeth, slightly larger than those in the first band (Figs 12B–E, 13B–C). Under PCM the second band is faintly visible in large as well as small specimens (Fig. 12B–E). The teeth of the third band are located within the posterior

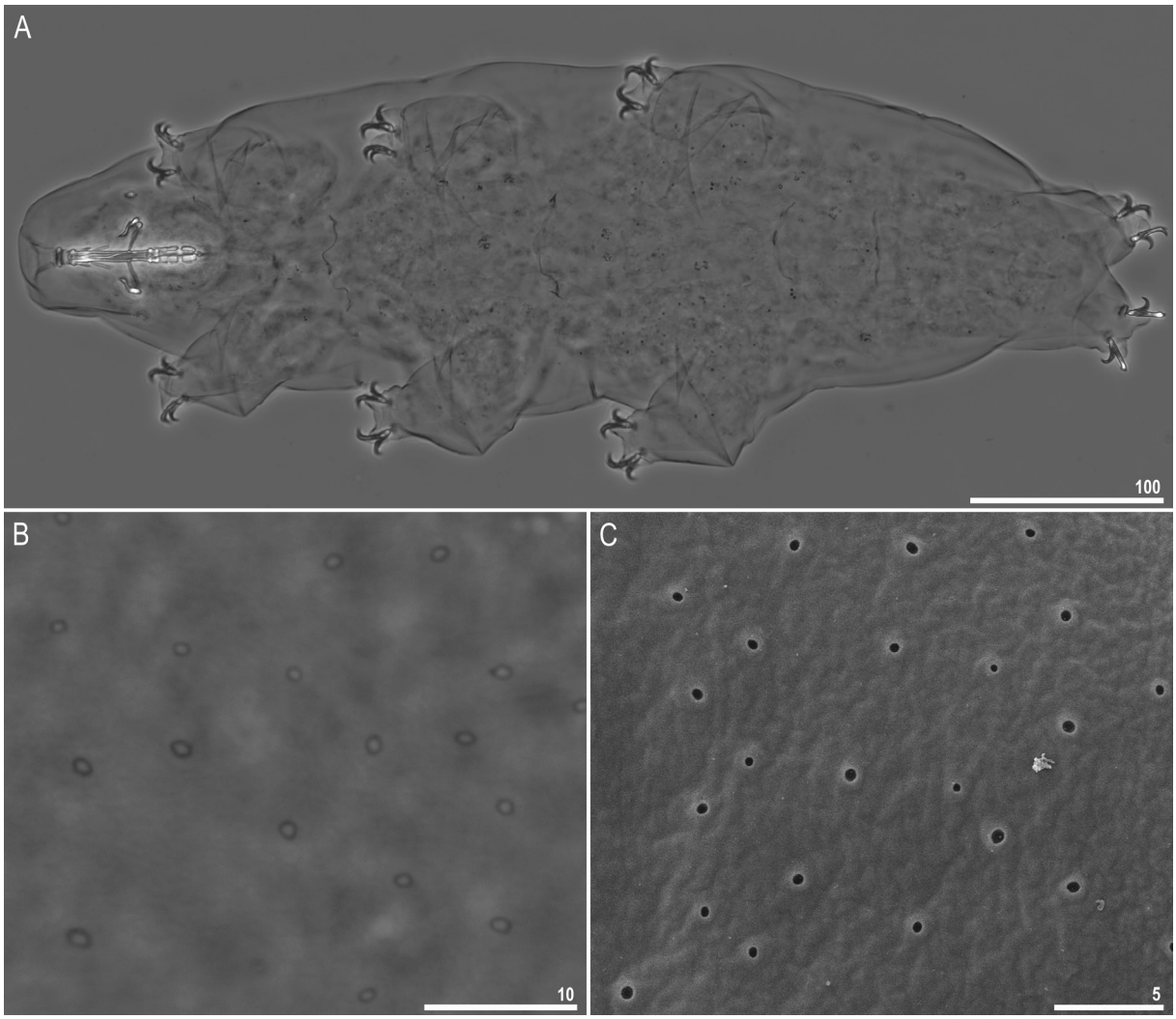


**Fig. 8.** *Macrobiotus kamilae* sp. nov., habitus. **A**. Dorso-ventral projection (holotype, Hoyer's medium, PCM, IZiBB IN.030.08). **B–C**. Cuticular pores on the dorsal part of the body seen in PCM (B: holotype) and in SEM (C: paratype, IZiBB). Scale bars in µm.

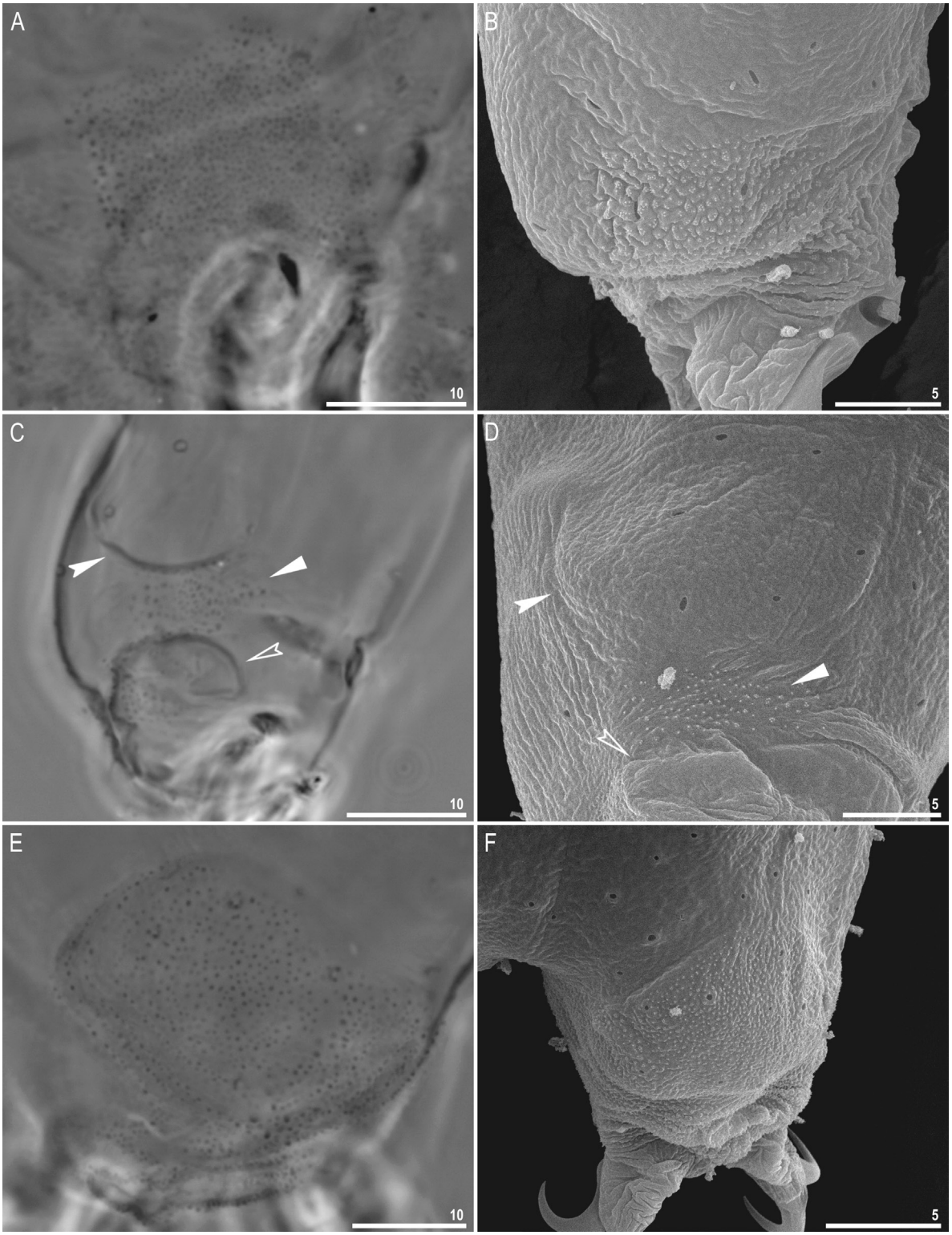


**Fig. 9.** *Macrobiotus kamilae* sp. nov., cuticular structures on legs (paratypes, IZiBB). **A–B**. External granulation on legs III and I seen in PCM (A) and SEM (B), respectively. **C–D**. A cuticular bulge (pulvinus), granulation and a cuticular fold on the internal surface of leg III seen in PCM (C) and SEM (D). **E–F**. Granulation on leg IV seen in PCM (E) and SEM (F). Filled indented arrowheads indicate the cuticular bulge, filled flat arrowheads indicate patch of granulation and empty indented arrowheads indicate the cuticular fold under the claws. Scale bars in μm.

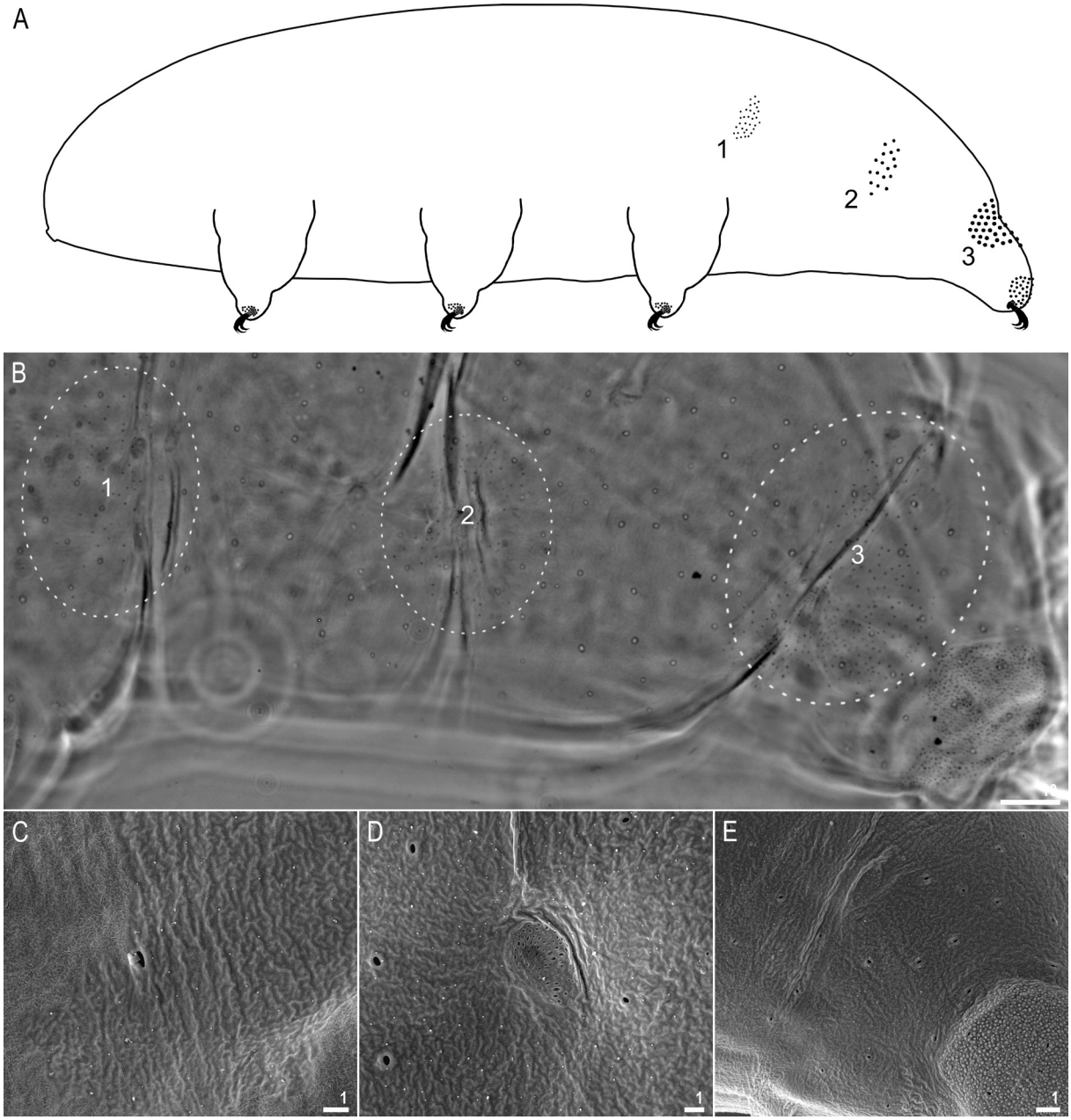


**Fig. 10.** *Macrobiotus kamilae* sp. nov., dorso-lateral patches of body granulation (paratypes, IZiBB). **A**. A semi-schematic drawing of a laterally positioned animal showing all patches of cuticular granulation: numbers indicate three dorso-lateral patches of body granulation (the granule sizes are not to scale, they have been enlarged in order to make them identifiable on the drawing). **B**. Three patches of dorso-lateral granulation visible in PCM. **C–E**. Magnifications of three patches of dorso-lateral granulation visible in SEM (C–E correspond to the patch numbers presented above). Please also note a cribriform area, which is external evidence of a muscle attachment in the centre of Fig. 10D. Scale bars in μm.

portion of the oral cavity, between the second band of teeth and the buccal tube opening (Figs 12B–E, 13B–C). The third band of teeth is discontinuous and divided into the dorsal and ventral portions. Under PCM, the dorsal teeth are fused and seen as one distinct transverse ridge, whereas the ventral teeth appear as two separate lateral transverse ridges and a median tooth which is sometimes divided into two roundish teeth (Fig. 12B–E). In SEM, both dorsal and ventral teeth are also clearly distinct (Fig. 13B–C). Under SEM, the margins of the dorsal portion of the third band are slightly serrated with two clearly visible peaks (Fig. 13B), whereas the ventral teeth are separated with a medio-ventral tooth slightly anterior to the lateral teeth (Fig. 13C). Pharyngeal bulb spherical, with triangular apophyses, two rod-shaped macroplacoids and a small triangular microplacoid (Fig. 12A, F–G). The macroplacoid length sequence 2 < 1. The first macroplacoid exhibits a central constriction, whereas the second macroplacoid is faintly sub-terminally constricted (Fig. 12F–G).

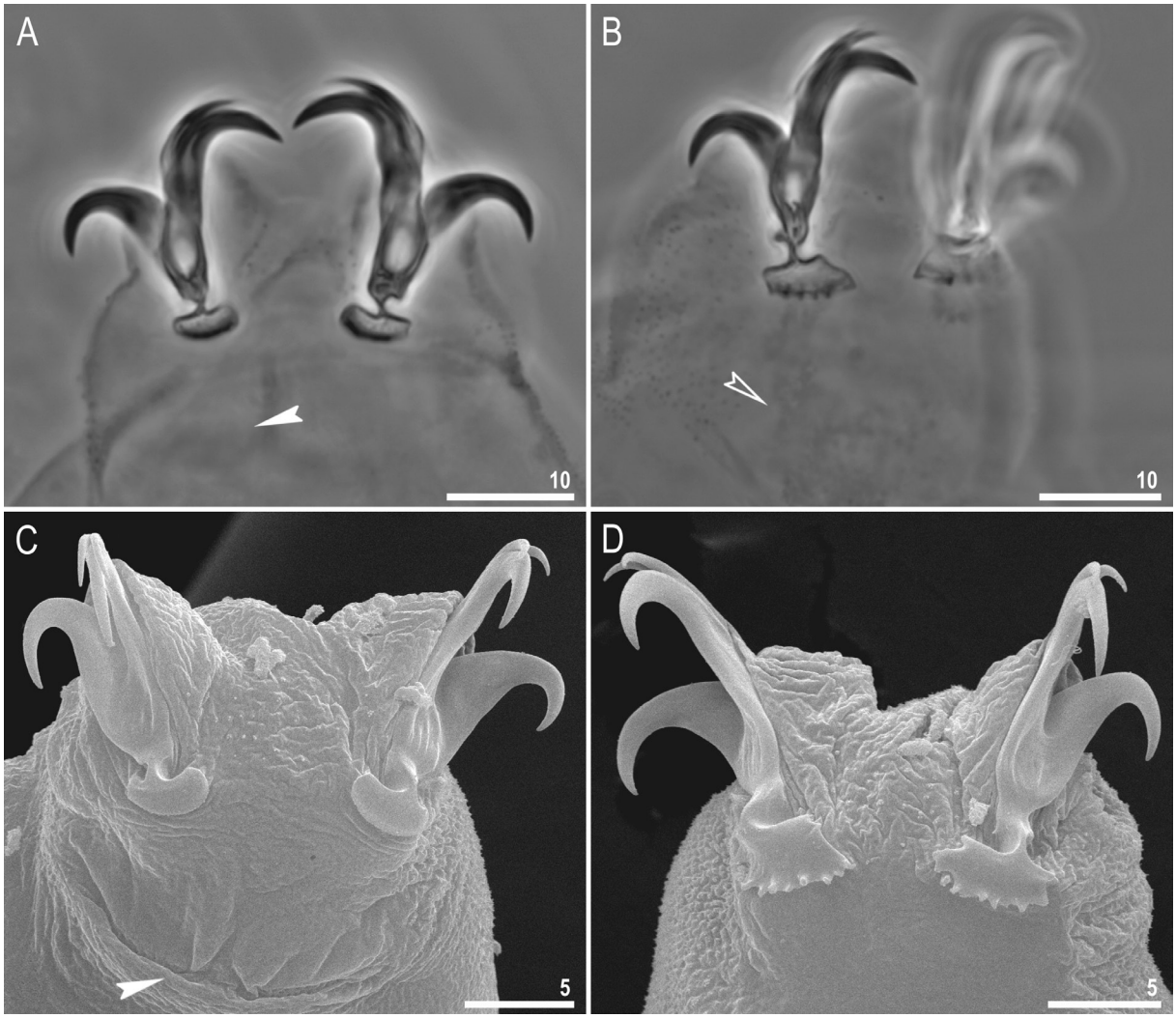


**Fig. 11.** *Macrobiotus kamilae* sp. nov., claws. **A–B**. Claws III and IV seen in PCM, with smooth and dentate lunules, respectively (holotype, IZiBB IN.030.08). **C–D**. Claws III and IV seen in SEM, with smooth and dentate lunules, respectively (paratype, IZiBB). Filled indented arrowheads indicate double muscle attachments under the claws whereas empty indented arrowhead indicates the horseshoe structure connecting the anterior and the posterior claw. Scale bars in μm.

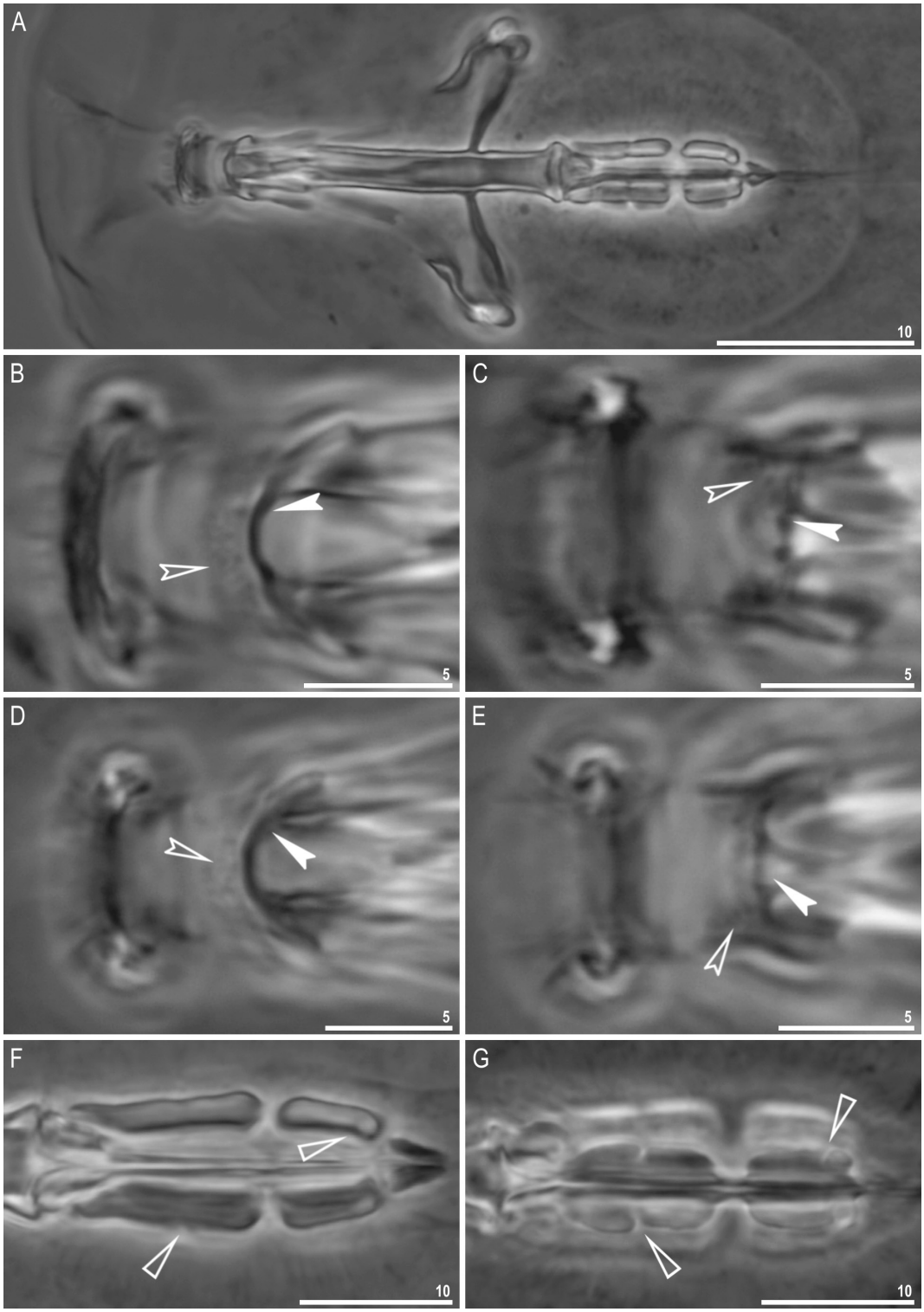


**Fig. 12.** *Macrobiotus kamilae* sp. nov., buccal apparatus and the oral cavity armature seen in PCM (paratypes, IZiBB). **A**. Dorso-ventral projection of the entire buccal apparatus. **B–E**. Oral cavity armature visible in dorsal (B, D) and ventral (C, E) views in a large and a small specimen, respectively. **F–G**. Placoid morphology visible in dorsal (F) and ventral (G) views, respectively. Empty indented arrowheads indicate the second band of teeth in the oral cavity, filled indented arrowheads indicate the third band of teeth in the oral cavity, whereas empty flat arrowheads indicate central constrictions in first macroplacoids and subterminal constriction in second macroplacoids. Scale bars in μm.

**Eggs** (measurements and statistics in Table 5)
Laid freely, yellowish, spherical or slightly ovoid (Figs 14A, 15A). The surface between processes is of the *hufelandi* type, i.e., covered with a reticulum (Figs 14E, 15B–F). Meshes of the reticulum small and rounded, irregular in size (mesh diameter 0.3–0.8 µm), with interbasal meshes slightly larger than peribasal meshes but peribasal meshes do not form rings around process bases (Figs 14E, 15B–F). The

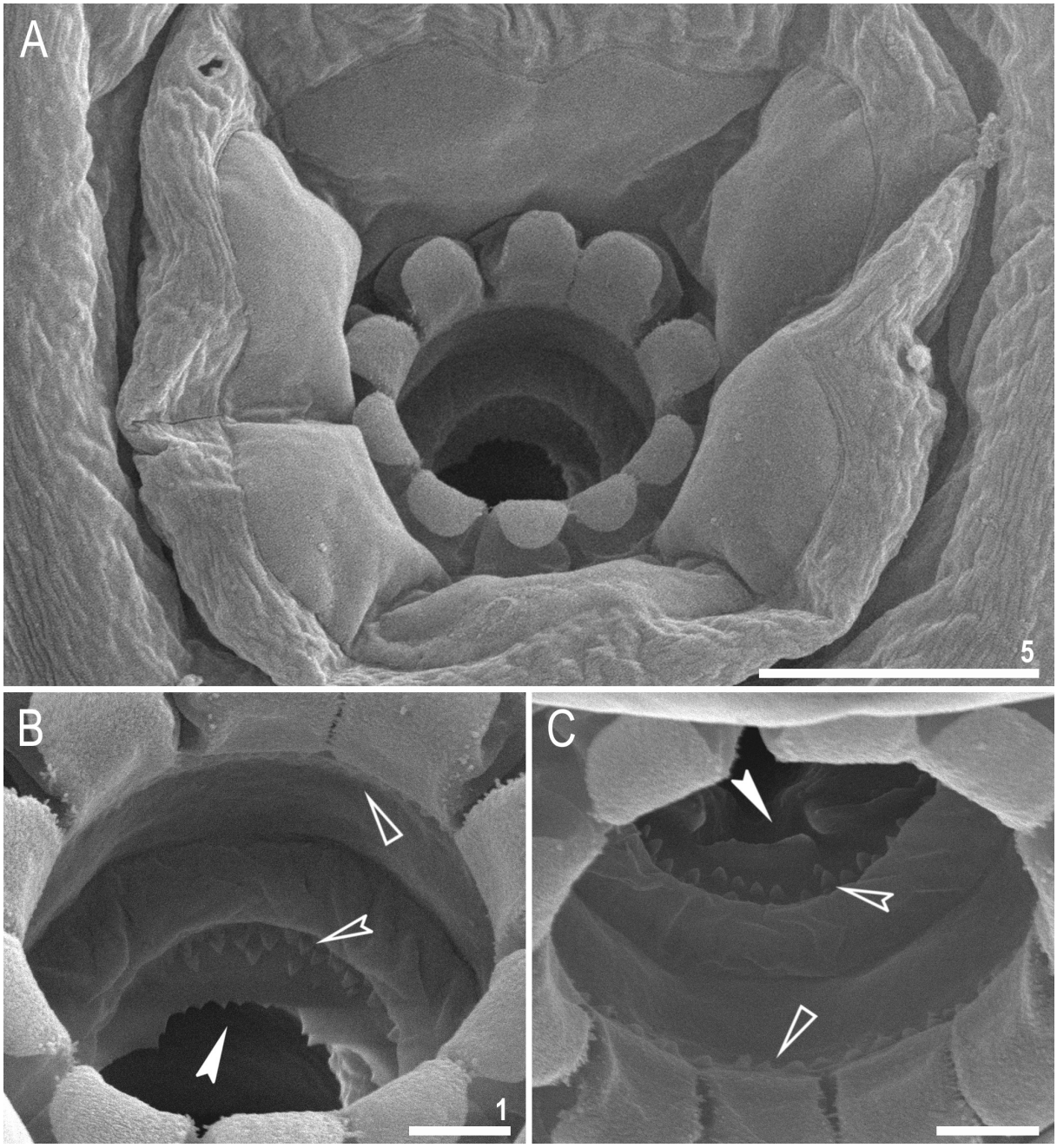


**Fig. 13.** *Macrobiotus kamilae* sp. nov., mouth opening and the oral cavity armature seen in SEM (paratype, IZiBB). **A**. Mouth opening with peribuccal sensory lobes and ten peribuccal lamellae. **B–C**. The oral cavity armature of a single paratype seen in SEM from different angles, in dorsal (B) and ventral (C) views, respectively. Empty flat arrowheads indicate the first band of teeth in the oral cavity, empty indented arrowheads indicate the second band of teeth in the oral cavity and filled indented arrowheads indicate the third band of teeth in the oral cavity. Scale bars in µm.

nodes of reticulum are often narrower than the mesh diameters visible in PCM and SEM (Figs 14E, 15F). Eggs have 26–32 processes on the circumference, 29 on average (Fig. 14A). Processes are of the inverted goblet shape with slightly concave trunks and concave terminal discs (Figs 14C–D, 15B–E). Terminal discs round, with faintly indented margins (Fig. 15B–E). Each terminal disc has a distinct

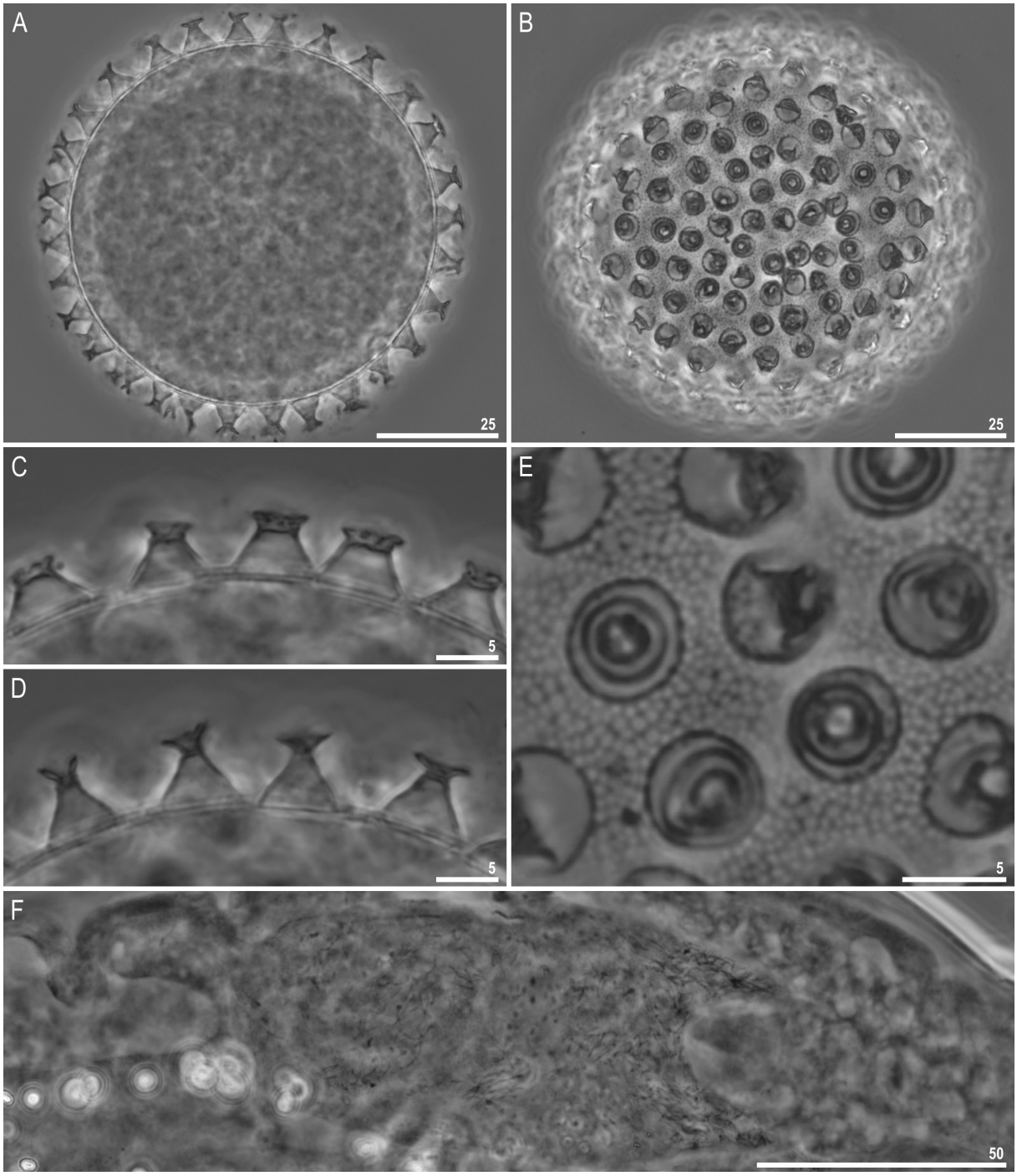


**Fig. 14.** *Macrobiotus kamilae* sp. nov. **A–E**. Egg seen in PCM (IZiBB). **A**. Midsection under 400× magnification. **B**. Surface under 400× magnification. **C–D**. Midsection under 1000× magnification. **E**. Surface under 1000× magnification. **F**. Male testis seen in PCM, with visible spermatozoa in a freshly mounted male in Hoyer's medium (paratype, IZiBB). Scale bars in μm.

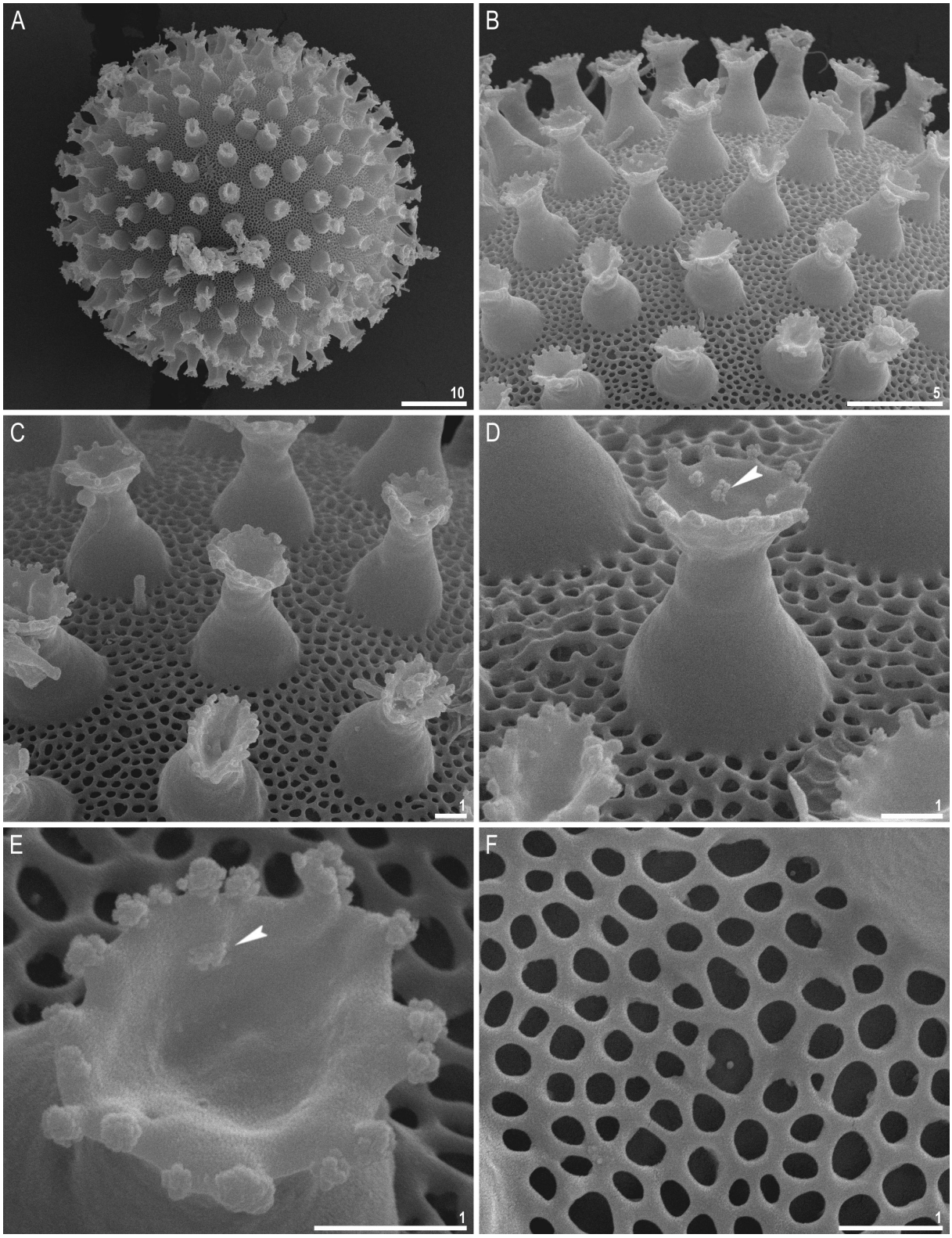


**Fig. 15.** *Macrobiotus kamilae* sp. nov., egg chorion morphology seen in SEM (IZiBB). **A**. Entire egg. **B–C**. Magnifications of the egg surface. **D**. Egg process morphology. **E**. Terminal disc. **F**. Details of the reticulation between egg processes. Arrowheads indicate scattered granules on the terminal disc surface. Scale bars in μm.

**Table 5.** Measurements (in μm) of selected morphological structures of the eggs of *Macrobiotus kamilae* sp. nov. mounted in Hoyer's medium (N = number of eggs/structures measured; Range = the smallest and the largest structure among all measured specimens; SD = standard deviation).

| Character | N | Range | MEAN | SD |
|---|---|---|---|---|
| Egg bare diameter | 30 | 65.0–90.6 | 77.4 | 5.5 |
| Egg full diameter | 30 | 74.9–102.5 | 87.6 | 6.0 |
| Process height | 90 | 4.1–7.7 | 5.6 | 0.8 |
| Process base width | 90 | 4.7–8.8 | 6.3 | 0.7 |
| Process base/height ratio | 90 | 76%–176% | 113% | 19% |
| Terminal disc width | 90 | 3.2–6.8 | 4.8 | 0.7 |
| Inter-process distance | 90 | 2.0–5.5 | 3.2 | 0.6 |
| Number of processes on egg circumference | 30 | 26–32 | 29.1 | 1.9 |

concave central area which may contain some scattered granulation within, which is also always present on the margin (visible only under SEM; Fig. 15E).

**Reproduction**

The new species is dioecious. No spermathecae filled with sperm have been found in gravid females on the freshly prepared slides. However, in males the testis, filled with spermatozoa, is clearly visible under PCM up to 24 hours after mounting in Hoyer's medium (Fig. 14F). The new species does not exhibit male secondary sexual dimorphism traits such as lateral gibbosities on legs IV.

**DNA sequences**

We obtained sequences for all four of the above-mentioned DNA markers. All sequenced fragments were represented by single haplotypes except the COI, in which two distinct haplotypes were present:

The 18S rRNA sequence (GenBank: MK737070), 1015 bp long.
The 28S rRNA sequence (GenBank: MK737064), 793 bp long.
The ITS-2 sequence (GenBank: MK737067), 381 bp long.
The COI haplotype 1 sequence (GenBank: MK737920), 658 bp long.
The COI haplotype 2 sequence (GenBank: MK737921), 658 bp long.

## *Phylogenetic analysis*

The phylogenetic analysis, based on available COI sequences of *M. hufelandi* spp., conducted in our study showed that *M. noongaris* sp. nov. and *M. kamilae* sp. nov. indeed belong to this group. The analysis recovered two highly supported clades (Fig. 16). The first grouping (blue nodes) is of species with typical processes of inverted goblet shape and whitish body (with the only exception being *M.* cf. *recens*, which has processes in the shape of thin cones devoid of terminal discs). In contrast to the first clade, the second group (red nodes) is of species with yellowish body and morphological modifications of egg processes (flexible filaments on the terminal discs or processes without terminal discs). Interestingly, the two new species described within this study, which both exhibit typical inverted goblet-shaped processes, have been found to cluster together with the species which have modified egg processes. However, *M. kamilae* sp. nov. has a yellowish body, which conforms to the second characteristic of this clade, whereas *M. noongaris* sp. nov. has a whitish body.

## Discussion

### Phenotypic differential diagnosis of *Macrobiotus noongaris* sp. nov.

In terms of the morphology of the animals, *M. noongaris* sp. nov., by having only the 2nd and 3rd bands of teeth in the oral cavity visible under PCM, belongs to the *patagonicus* subgroup within the *M. hufelandi* complex. However, regarding egg shell ornamentation, by having the egg shell surface between the processes covered with a reticulum, it represents the *hufelandi* subgroup. These two traits combined with the typical concave terminal discs with serration/dentation make *M. noongaris* sp. nov. most similar to the following species: *M. horningi* Kaczmarek & Michalczyk, 2017, *M. sandrae* Bertolani & Rebecchi, 1993, *M. sottilei* Pilato, Kiosya, Lisi & Sabella, 2012, *M. terminalis* Bertolani & Rebecchi, 1993 and *M. vladimiri* Bertolani, Biserov, Rebecchi & Cesari, 2011, but it differs specifically in the following aspects.

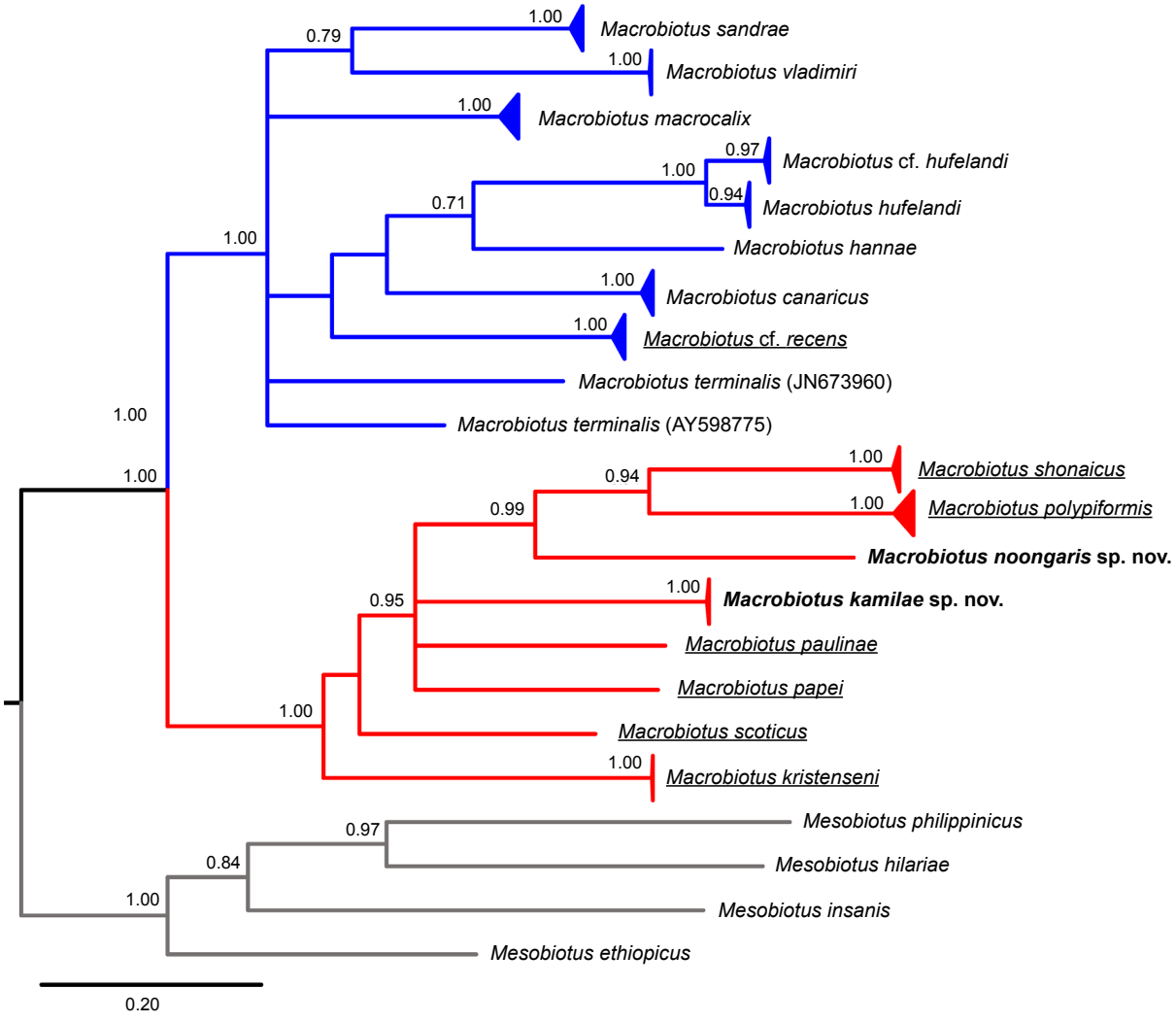


**Fig. 16.** The Bayesian Inference (BI) phylogeny constructed from COI sequences of the *Macrobiotus hufelandi* group species. Numbers at nodes indicate Bayesian posterior probability. Two previously recognized clades, one grouping mostly species with typical inverted goblet-shaped processes and the second grouping mostly species with morphological modifications of egg processes, are marked in blue and red, respectively. Species of the *hufelandi* group with atypical egg processes are indicated by underlined font. Please see Appendix 1 for details on species sequences used in the analysis. The outgroup is marked with grey. The scale bar represents substitutions per position.

It differs from *M. horningi*, reported only from its type locality in New Zealand (Kaczmarek & Michalczyk 2017b), by the presence of granulation on all legs (poorly visible granulation present only on legs IV in *M. horningi*), the presence of clearly visible subterminal constrictions in the second macroplacoid (only a poorly defined latero-terminal globular projection in the second macroplacoid in *M. horningi*), the morphology of lunules IV (dentate in the new species vs smooth in *M. horningi*), a smaller mesh size in the reticulum on the egg surface (mesh diameter: 0.1–0.6 μm in the new species vs 1.0–1.8 μm in *M. horningi*), a different location of larger meshes within the reticulum (interbasal meshes larger than peribasal meshes in the new species vs peribasal meshes slightly larger than the interbasal mesh in *M. horningi*), the morphology of terminal disc margins (strongly serrated in the new species vs well-defined indentations in *M. horningi*) and by smaller egg process dimensions (height 4.5–8.4 μm, base width 3.4–6.6 μm, disc diameter 2.3–4.8 μm in the new species vs height 11.8–13.3 μm, base width 8.2–8.6 μm and disk diameter 6.0–6.6 μm in *M. horningi*).

It differs from *M. sandrae*, reported from its type locality in Germany and also Italy (Bertolani & Rebecchi 1993) and from Belarus (Pilato *et al.* 2012), by the presence of a clearly visible subterminal constriction in the second macroplacoid (no constriction in *M. sandrae*), the presence of microgranulation on the margins of terminal discs of egg processes (the microgranulation absent in *M. sandrae*) and by a different morphology of the reticulation on the egg surface (slightly smaller mesh size (0.1–0.6 μm), several rows of meshes in the reticulum between processes, mesh rims often wider than pore diameter, meshes almost circular in the new species vs bigger mesh size (0.6–1.0 μm), often only up to three rows of pores in the reticulum between processes, mesh rims clearly thinner than pore diameter and meshes more ovoid in *M. sandrae*).

It differs from *M. sottilei*, known from its type locality in Belarus (Pilato *et al.* 2012) but also from Poland (Kaczmarek *et al.* 2018) and Italy (Roszkowska *et al.* 2019), by the presence of three distinct teeth/ridges in the dorsal portion of the third band of teeth (the teeth/ridges of the dorsal portion fused and form a continuous arc in *M. sottilei*) and by a slightly more posterior stylet support insertion point (*pt = 76.7–81.6* in the new species vs *75.3–76.6* in *M. sottilei*).

It differs from *M. terminalis*, known from its type locality in Italy (Bertolani & Rebecchi 1993) and from Belarus (Pilato *et al.* 2012), by the morphology of lunules I–III (smooth in the new species vs dentate in *M. terminalis*), a different morphology of the reticulation on the egg surface (smaller mesh size (0.1–0.6 μm), several rows of meshes in the reticulum between processes, mesh rims often wider than pore diameter and meshes almost circular in the new species vs bigger mesh size (0.8–1.3 μm), often only up to three rows of pores in the reticulum between processes, mesh rims clearly thinner than pore diameter and meshes more ovoid in *M. terminalis*) and by the presence of microgranulation on the margins of terminal discs of egg processes (absent in *M. terminalis*).

It differs from *M. vladimiri*, known from its type locality in Italy and from Germany (Bertolani *et al.* 2011b; originally listed as *M.* cf. *terminalis* in Bertolani & Rebecchi (1993)), Poland (Nowak & Stec 2017) and Spain (Bertolani *et al.* 2011a), by a different morphology of the reticulation on the egg surface (smaller mesh size (0.1–0.6 μm), several rows of meshes between processes, meshes distributed uniformly, mesh rims often wider than mesh diameter and meshes almost circular in the new species vs bigger mesh size (0.8–1.1 μm), often only up to three rows of meshes between processes, clear peribasal of larger meshes, mesh rims clearly thinner than mesh diameter and meshes more ovoid in *M. vladimiri*), the presence of microgranulation on the margins of terminal discs of egg processes (absent in *M. vladimiri*) and by reproductive mode (dioecism in the new species vs parthenogenesis in *M. vladimiri*).

**Genotypic differential diagnosis of *Macrobiotus noongaris* sp. nov.**

The ranges of uncorrected genetic p-distances between the new species and species of the *M. hufelandi* complex, for which sequences are available from GenBank, are as follows (from the most to the least conservative):

- 18S rRNA: 0.4–3.5% (2.0% on average), with the most similar being an undetermined *M. hufelandi* group species from Italy and *M. papei* from Tanzania (HQ604971 and MH063881, respectively) and the least similar being *Macrobiotus polonicus* Pilato, Kaczmarek, Michalczyk & Lisi, 2003 from Poland (HM187580);
- 28S rRNA: 3.8–10.2% (8.0% on average), with the most similar being *M. papei* from Tanzania (MH063880) and the least similar being *Macrobiotus macrocalix* Bertolani & Rebecchi, 1993 from Poland (MH063935);
- COI: 20.0–25.2% (22.6% on average), with the most similar being *M. shonaicus* from Japan (MG757136) and the least similar being *M. canaricus* from Spain (MH057765);
- ITS-2: 9.4–30.2% (21.1% on average), with the most similar being *Macrobiotus sapiens* Binda & Pilato, 1984 from Croatia (GQ403680) and the least similar being *M.* cf. *recens* from Spain (MH063932).

**Phenotypic differential diagnosis of *Macrobiotus kamilae* sp. nov.**

*Macrobiotus kamilae* sp. nov., by the presence of patches of cuticular granulation on the body in areas other than the legs, is similar to two species of the *M. hufelandi* complex namely, *M. papei* and *M. paulinae* Stec, Smolak, Kaczmarek & Michalczyk, 2015. However, it differs specifically in the following aspects.

It differs from *M. papei*, reported only from its type locality in Tanzania (Stec *et al.* 2018d), by the presence of three dorso-lateral patches of granulation on the body (only one patch of granulation just above the granulation on legs IV present in *M. papei*), the depth of constrictions in the macroplacoids (well-defined in the new species vs poorly defined in *M. papei*), a slightly more posterior stylet support insertion point (*pt = 76.7–81.6* in the new species vs *pt = 72.4–76.4* in *M. papei*), the terminal disc morphology (with indented margins in the new species vs with flexible filaments in *M. papei*) and by the reproductive mode (dioecism in the new species vs parthenogenesis in *M. papei*).

It differs from *M. paulinae*, reported only from its type locality in Kenya (Stec *et al.* 2015; McInnes *et al.* 2017), by the type of oral cavity armature (*patagonicus* type in the new species vs *maculatus* type in *M. paulinae*), the number of dorso-lateral patches of granulation on the body (three in the new species vs seven in *M. paulinae*), the number of granulation patches on the external surface of legs I–III (one in the new species vs two in *M. paulinae*), slightly more posteriorly positioned stylet support insertion point (*pt = 76.7–81.6* in the new species vs *pt = 69.7–75.0* in *M. papei*) and by the morphology of terminal discs of egg processes (with indented margins in the new species vs with flexible filaments in *M. papei*).

**Genotypic differential diagnosis of *Macrobiotus kamilae* sp. nov.**

The ranges of uncorrected genetic p-distances between the new species and species of the *M. hufelandi* complex, for which sequences are available from GenBank, are as follows (from the most to the least conservative):

- 18S rRNA: 1.3–4.4% (2.3% on average), with the most similar being an undetermined *M. hufelandi* group species from Italy and *M. papei* from Tanzania (HQ604971 and MH063881, respectively) and the least similar being *M. polonicus* from Poland (HM187580);
- 28S rRNA: 3.6–10.3% (8.1% on average), with the most similar being *M. paulinae* from Kenya (MH063880) and the least similar being *M. macrocalix* from Poland (MH063935);

- COI: 21.1–24.8% (23.8% on average), with the most similar being *Macrobiotus polypiformis* Roszkowska, Ostrowska, Stec, Janko & Kaczmarek, 2017 from Ecuador (KX810011) and the least similar being *M. terminalis* from Italy (JN673960);
- ITS-2: 13.4–33.7% (23.3% on average), with the most similar being *M. paulinae* from Kenya and *M. noongaris* sp. nov. from Australia (KT935500 and MK737066, respectively) and the least similar being *Macrobiotus scoticus* Stec, Morek, Gąsiorek, Blagden & Michalczyk, 2017 from Scotland (KY797268).

**Phylogeny of the *Macrobiotus hufelandi* complex**

The first attempt to investigate the phylogeny of the *M. hufelandi* complex was presented by Guidetti *et al.* (2013) along with the description of the new species, *Macrobiotus kristenseni* Guidetti, Peluffo, Rocha, Cesari & Moly de Peluffo, 2013, which exhibits egg processes atypical for this group. First, they provided an unrooted neighbour joining dendrogram based on COI sequences showing high genetic divergences between eight *M. hufelandi* species for which these fragments had been available (Guidetti *et al.* 2005; Cesari *et al.* 2009; Bertolani *et al.* 2011a, 2011b). Second, they also presented phylogeny based on a conservative marker (18S rRNA), showing undoubtedly that, although the new species possesses modified egg processes, it still belongs to the *M. hufelandi* complex. Thus, Guidetti *et al.* (2013) hypothesised that within this group, animal morphology is more conserved than the morphology of egg ornamentation. Since then, several new species with modified egg process morphology have been discovered and described by means of integrative taxonomy (Stec *et al.* 2015, 2017b; Roszkowska *et al.* 2017). Soon after this, along with the description of another new species, *M. shonaicus*, Stec *et al.* (2018a) provided an upgraded COI phylogeny of the complex and discovered two well-supported evolutionary lineages. This diversification was congruent with the morphology, as one clade comprised species with a whitish body and the typical inverted goblet-shaped processes whereas the second one grouped species with a yellowish body and egg processes with a modified morphology (conical processes or processes with filaments growing out of terminal discs). The presence of these two evolutionary lineages was then confirmed by Stec *et al.* (2018b), who provided three congruent phylogenies based on different data sets for the *M. hufelandi* complex (1: 18S rRNA; 2: 18S rRNA+28S rRNA+ITS2+COI; 3: COI). However, *Macrobiotus* cf. *recens* (with a whitish body and conical egg processes) analysed in that study, was found to be embedded within the clade with species exhibiting the typical egg morphology. Nevertheless, these two clades still could be morphologically differentiated by the body colour, whitish vs yellowish, respectively. Although *M. noongaris* sp. nov. and *M. kamilae* sp. nov., described in our study, do not exhibit modified egg processes, both of them have been recovered as members of the clade with such eggs. Notably, however, only *M. kamilae* sp. nov. by having a yellowish body conforms to the second characteristic of this clade, whereas *M. noongaris* sp. nov. contradicts the hypothesis proposed by Stec *et al.* (2018a, 2018b). These results indicate explicitly that diversification of egg shell ornamentation is definitely faster evolving than animal morphology, a hypothesis which was already presented by Guidetti *et al.* (2013). Furthermore, this is also in line with a previous study conducted on a more detailed and targeted scale by Stec *et al.* (2016b), who showed congruence between genetic and phenotypic traits of the eggs within a single parthenogenetic tardigrade species. The authors stated that this divergence between two reproductively isolated lineages could be seen as an example of very early incipient speciation. Hopefully, in the near future the phylogenetic data set will be extended by the addition of more *M. hufelandi* complex species, which can definitely contribute to our understanding of the morphological evolution within this group.

**Conclusions**

Our study integratively describes two new species of the cosmopolitan tardigrade group, the *M. hufelandi* complex, and contributes to the understanding of its evolution. The phylogenetic analysis showed that these new species, having the typical inverted goblet-shaped processes on the eggs, cluster together

with species exhibiting morphological modifications of the egg processes. This contradicts the previous hypothesis that two well-supported evolutionary lineages within the *M. hufelandi* complex differ by egg chorion ornamentation. However, our results are in line with the hypothesis presented by Guidetti *et al.* (2013) that animal morphology is much more conserved that egg chorion ornamentation, where the latter provide the most important characters for species diagnosis and identification. Finally, we would like to note that *M. noongaris* sp. nov. is the third and *M. kamilae* sp. nov. the first formally described species of *M. hufelandi* complex from Australia and India, respectively.

## Acknowledgements

We are very grateful to Łukasz Michalczyk, who collected the sample in Australia and to Krzysztof Miler for the moss sample from India, in which we have discovered the two new species. We would also like to thank Ryan Głowacki, Bushland Manager for the Botanic Gardens and Parks Authority (Kings Park, Perth, Australia), for his valuable assistance in sampling in Western Australia (collection permit no. SW016900 to ŁM). We are also grateful to both our reviewers, Diane Nelson and Łukasz Kaczmarek, as well as to ŁM for suggestions and linguistic corrections which improved our work. We would like to thank Łukasz Krzywański, who helped with the assembly of morphological figures. We would also like to thank to the Aquatic Ecosystems Group (Institute of Environmental Sciences, Jagiellonian University, Poland) for providing us with rotifers. The study was supported by the Polish National Science Centre via the 'Sonata Bis' programme (grant no. 2016/22/E/NZ8/00417 awarded to ŁM).

## References

Abe W. & Takeda M. 2000. A new record of *Cornechiniscus madagascariensis* Maucci, 1993 (Tardigrada: Echiniscidae) from India. *Proceedings of the Biological Society of Washington* 113: 480–485.

Bertolani R. & Rebecchi L. 1993. A revision of the *Macrobiotus hufelandi* group (Tardigrada, Macrobiotidae), with some observations on the taxonomic characters of eutardigrades. *Zoologica Scripta* 22: 127–152. https://doi.org/10.1111/j.1463-6409.1993.tb00347.x

Bertolani R., Rebecchi L., Giovannini I. & Cesari M. 2011a. DNA barcoding and integrative taxonomy of *Macrobiotus hufelandi* C.A.S. Schultze 1834, the first tardigrade species to be described, and some related species. *Zootaxa* 2997: 19–36. https://doi.org/10.11646/zootaxa.2997.1.2

Bertolani R., Biserov V., Rebecchi L. & Cesari M. 2011b. Taxonomy and biogeography of tardigrades using an integrated approach: new results on species of the *Macrobiotus hufelandi* group. *Invertebrate Zoology* 8 (1): 23–36. https://doi.org/10.15298/invertzool.08.1.05

Bertolani R., Guidetti R., Marchioro T., Altiero T., Rebecchi L. & Cesari M. 2014. Phylogeny of Eutardigrada: New molecular data and their morphological support lead to the identification of new evolutionary lineages. *Molecular Phylogenetics and Evolution* 76: 110–126. https://doi.org/10.1016/j.ympev.2014.03.006

Biserov V.I. 1990a. On the revision of the genus *Macrobiotus*. The subgenus *Macrobiotus* s. str.: a new systematic status of the group *hufelandi* (Tardigrada, Macrobiotidae). Communication 1. *Zoologicheskii Zhurnal* 69 (12): 5–17. [In Russian.]

Biserov V.I. 1990b. On the revision of the genus *Macrobiotus*. The subgenus *Macrobiotus* s. str.: a new systematic status of the group *hufelandi* (Tardigrada, Macrobiotidae). Communication 2. *Zoologicheskii Zhurnal* 69 (12): 38–50. [In Russian.]

Campbell L.I., Rota-Stabelli O., Edgecombe G.D., Marchioro T., Longhorn S.J., Telford M.J., Philippe H., Rebecchi L., Peterson K.J. & Pisani D. 2011. MicroRNAs and phylogenomics resolve the relationships of Tardigrada and suggest that velvet worms are the sister group of Arthropoda. *Proceedings of the National Academy of Sciences* 108 (38): 15920–15924. https://doi.org/10.1073/pnas.1105499108

Casquet J.T., Thébaud C. & Gillespie R.G. 2012. Chelex without boiling, a rapid and easy technique to obtain stable amplifiable DNA from small amounts of ethanol-stored spiders. *Molecular Ecology Resources* 12: 136–141. https://doi.org/10.1111/j.1755-0998.2011.03073.x

Cesari M., Bertolani R., Rebecchi L. & Guidetti R. 2009. DNA barcoding in Tardigrada: the first case study on *Macrobiotus macrocalix* Bertolani & Rebecchi 1993 (Eutardigrada, Macrobiotidae). *Molecular Ecology Resources* 9 (3): 699–706. https://doi.org/10.1111/j.1755-0998.2009.02538.x

Cesari M., Giovanni I., Bertolani R. & Rebecchi L. 2011. An example of problems associated with DNA barcoding in tardigrades: a novel method for obtaining voucher specimens. *Zootaxa* 3104: 42–51.

Claxton S.K. 2004. *The Taxonomy and Distribution of Australian Terrestrial Tardigrades*. PhD thesis, *Macquire University, Sydney*.

Dastych H. 1980. Niesporczaki (Tardigrada) Tatrzańskiego Parku Narodowego. *Monografie Fauny Polski* 9: 1–232.

Degma P. & Guidetti R. 2007. Notes to the current checklist of Tardigrada. *Zootaxa* 1579: 41–53. https://doi.org/10.11646/zootaxa.1579.1.2

Degma P., Bertolani R. & Guidetti R. 2009–2019. Actual checklist of Tardigrada species (2009–2019, 35t$^{h}$ Edition: 31-07-2019): 48. Available from http://www.tardigrada.modena.unimo.it/miscellanea/Actual%20checklist%20of%20Tardigrada.pdf [accessed 29 Jul. 2019].

Dey P.K. & Mandal K. 2018. Tardigrada. *In*: Chandra K., Gupta D., Gopi K.C., Tripathy B. & Kumar V. (eds) *Faunal Diversity of Indian Himalaya*: 779–783. Zoological Survey of India, Kolkata.

Durante Pasa M.V. & Maucci W. 1979. Tardigrada muscicolo della Grecia. *Zeszyty Naukowe Uniwersytetu Jagiellońskiego Prace Zoologiczne* 25: 19–45.

Folmer O., Black M., Hoeh W., Lutz R. & Vrijenhoek R. 1994. DNA primers for amplification of mitochondrial cytochrome c oxidase subunit I from diverse metazoan invertebrates. *Molecular Marine Biology and Biotechnology* 3: 294–299.

Gąsiorek P. & Michalczyk Ł. 2019. *Echiniscus siticulosus* (Echiniscidae: *spinulosus* group), a new tardigrade from Western Australian scrub. *New Zealand Journal of Zoology*. https://doi.org/10.1080/03014223.2019.1603166

Gąsiorek P., Stec D., Zawierucha Z., Kristensen R.M. & Michalczyk Ł. 2018. Revision of *Testechiniscus* Kristensen, 1987 (Heterotardigrada: Echiniscidae) refutes the polar-temperate distribution of the genus. *Zootaxa* 4472 (2): 261–297. https://doi.org/10.11646/zootaxa.4472.2.3

Giribet G., Carranza S., Baguña J., Riutort M. & Ribera C. 1996. First molecular evidence for the existence of a Tardigrada + Arthropoda clade. *Molecular Biology and Evolution* 13: 76–84. https://doi.org/10.1093/oxfordjournals.molbev.a025573

Guidetti R. & Bertolani R. 2005. Tardigrade taxonomy: an updated check list of the taxa and a list of characters for their identification. *Zootaxa* 845: 1–46. https://doi.org/10.11646/zootaxa.845.1.1

Guidetti R., Gandolfi A., Rossi V. & Bertolani R. 2005. Phylogenetic analysis of Macrobiotidae (Eutardigrada, Parachela): a combined morphological and molecular approach. *Zoologica Scripta* 34: 235–244. https://doi.org/10.1111/j.1463-6409.2005.00193.x

Guidetti R., Peluffo J.R., Rocha A.M., Cesari M. & Moly de Peluffo M.C. 2013. The morphological and molecular analyses of a new South American urban tardigrade offer new insights on the biological meaning of the *Macrobiotus hufelandi* group of species (Tardigrada: Macrobiotidae). *Journal of Natural History* 47 (37–38): 2409–2426. https://doi.org/10.1080/00222933.2013.800610

Guil N. & Giribet G. 2012. A comprehensive molecular phylogeny of tardigrades – adding genes and taxa to a poorly resolved phylum-level phylogeny. *Cladistics* 28 (1): 21–49. https://doi.org/10.1111/j.1096-0031.2011.00364.x

Guil N., Jørgensen A. & Kristensen R. 2019. An upgraded comprehensive multilocus phylogeny of the Tardigrada tree of life. *Zoologica Scripta* 48 (1): 120–137. https://doi.org/10.1111/zsc.12321

Hall T.A. 1999. BioEdit: a user-friendly biological sequence alignment editor and analysis program for Windows 95/98/NT. *Nucleic Acids Symposium Series* 41: 95–98.

Iharos G. 1969. Beiträge zur Kenntnis der Tardigraden Indiens. *Opuscola Zoologica, Budapest* 9 (1): 107–113.

Jørgensen A., Møbjerg N. & Kristensen R.M. 2007. A molecular study of the tardigrade *Echiniscus testudo* (Echiniscidae) reveals low DNA sequence diversity over a large geographical area. *Journal of Limnology* 66: 77–83. https://doi.org/10.4081/jlimnol.2007.s1.77

Kaczmarek Ł. & Michalczyk Ł. 2017a. The *Macrobiotus hufelandi* (Tardigrada) group revisited. *Zootaxa* 4363: 101–123. https://doi.org/10.11646/zootaxa.4363.1.4

Kaczmarek Ł. & Michalczyk Ł. 2017b. A description of *Macrobiotus horningi* sp. nov. and redescriptions of *M. maculatus* comb. nov. Iharos, 1973 and *M. rawsoni* Horning *et al.*, 1978 (Tardigrada: Eutardigrada: Macrobiotidae: *hufelandi* group). *Zootaxa* 4363: 79–100. https://doi.org/10.11646/zootaxa.4363.1.3

Kaczmarek Ł., Michalczyk Ł. & McInnes S.J. 2014a. Annotated zoogeography of non-marine Tardigrada. Part I: Central America. *Zootaxa* 3763: 1–62. https://doi.org/10.11646/zootaxa.3763.1.1

Kaczmarek Ł., Cytan J., Zawierucha K., Diduszko D. & Michalczyk Ł. 2014b. Tardigrades from Peru (South America), with descriptions of three new species of Parachela. *Zootaxa* 3790: 357–379. https://doi.org/10.11646/zootaxa.3790.2.5

Kaczmarek Ł., Michalczyk Ł. & McInnes S.J. 2015. Annotated zoogeography of non-marine Tardigrada. Part II: South America. *Zootaxa* 3923: 1–107. https://doi.org/10.11646/zootaxa.3923.1.1

Kaczmarek Ł., Michalczyk Ł. & McInnes S.J. 2016. Annotated zoogeography of non-marine Tardigrada. Part III: North America and Greenland. *Zootaxa* 4203: 1–249. https://doi.org/10.11646/zootaxa.4203.1.1

Kaczmarek Ł., Kosicki J.Z. & Roszkowska M. 2018. Tardigrada of Bory Tucholskie National Park, Zaborski Landscape Park, and their surroundings (Pomerania Province, Poland). *Turkish Journal of Zoology* 42: 6–17. https://doi.org/10.3906/zoo-1705-44

Katoh K. & Toh H. 2008. Recent developments in the MAFFT multiple sequence alignment program. *Briefings in Bioinformatics* 9: 286–298. https://doi.org/10.1093/bib/bbn013

Katoh K., Misawa K., Kuma K. & Miyata T. 2002. MAFFT: a novel method for rapid multiple sequence alignment based on fast Fourier transform. *Nucleic Acids Research* 30: 3059–66. https://doi.org/10.1093/nar/gkf436

Kristensen R.M. 1987. Generic revision of the Echiniscidae (Heterotardigrada), with a discussion of the origin of the family. *In*: Bertolani R. (ed.) *Biology of Tardigrada*: 261–335. Selected Symposia and Monographs, U.Z.I., Mucchi, Modena.

Kumar S., Stecher G. & Tamura K. 2016. MEGA7: Molecular Evolutionary Genetics Analysis version 7.0 for bigger datasets. *Molecular Biology and Evolution* 33: 1870–1874. https://doi.org/10.1093/molbev/msw054

Lanfear R., Frandsen P.B., Wright A.M., Senfeld T. & Calcott B. 2016. PartitionFinder 2: new methods for selecting partitioned models of evolution for molecular and morphological phylogenetic analyses. *Molecular Biology and Evolution* 34: 772–773. https://doi.org/10.1093/molbev/msw260

Mapalo M., Stec D., Mirano-Bascos D.M. & Michalczyk Ł. 2016. *Mesobiotus philippinicus* sp. nov., the first limnoterrestrial tardigrade from the Philippines. *Zootaxa* 4126 (3): 411–426. https://doi.org/10.11646/zootaxa.4126.3.6

Mapalo M., Stec D., Mirano-Bascos D.M. & Michalczyk Ł. 2017. An integrative description of a limnoterrestrial tardigrade from the Philippines, *Mesobiotus insanis*, new species (Eutardigrada: Macrobiotidae: *harmsworthi* group). *Raffles Bulletin of Zoology* 65: 440–454.

Maucci W. 1979. I *Pseudechiniscus* del gruppo *cornutus* con descrizione di una nuova specie (Tardigrada, Echiniscidae). *Zeszyty Naukowe Uniwersytetu Jagiellońskiego, Prace Zoologiczne* 25: 107–124.

Maucci W. & Durante Pasa M.V. 1980. Tardigradi muscicoli delle Isole Andamane. *Bollettino Museo Civico di Storia Naturale di Verona* 7: 281–291.

McInnes S.J. 1994. Zoogeographic distribution of terrestrial/freshwater tardigrades from current literature. *Journal of Natural History* 28 (2): 257–352. https://doi.org/10.1080/00222939400770131

McInnes S.J., Michalczyk Ł. & Kaczmarek Ł. 2017. Annotated zoogeography of non-marine Tardigrada. Part IV: Africa. *Zootaxa* 4284: 1–71. https://doi.org/10.11646/zootaxa.4284.1.1

Michalczyk Ł. & Kaczmarek Ł. 2003. A description of the new tardigrade *Macrobiotus reinhardti* (Eutardigrada, Macrobiotidae, *harmsworthi* group) with some remarks on the oral cavity armature within the genus *Macrobiotus* Schultze. *Zootaxa* 331: 1–24. https://doi.org/10.11646/zootaxa.331.1.1

Michalczyk Ł. & Kaczmarek Ł. 2013. The Tardigrada Register: a comprehensive online data repository for tardigrade taxonomy. *Journal of Limnology* 72: 175–181. https://doi.org/10.4081/jlimnol.2013.s1.e22

Michalczyk Ł., Wełnicz W., Frohme M. & Kaczmarek Ł. 2012. Redescriptions of three *Milnesium* Doyère, 1840 taxa (Tardigrada: Eutardigrada: Milnesiidae), including the nominal species for the genus. *Zootaxa* 3154: 1–20. https://doi.org/10.11646/zootaxa.3154.1.1

Mironov S.V., Dabert J. & Dabert M. 2012. A new feather mite species of the genus *Proctophyllodes* Robin, 1877 (Astigmata: Proctophyllodidae) from the Long-tailed Tit *Aegithalos caudatus* (Passeriformes: Aegithalidae): morphological description with DNA barcode data. *Zootaxa* 3253: 54–61. https://doi.org/10.11646/zootaxa.3253.1.2

Morek W., Stec D., Gąsiorek P., Schill R.O., Kaczmarek Ł. & Michalczyk Ł. 2016. An experimental test of eutardigrade preparation methods for light microscopy. *Zoological Journal of the Linnean Society* 178: 785–793. https://doi.org/10.1111/zoj.12457

Morgan C.I. & Nicholls C.A. 1986. *Apodibius serventyi* sp. nov., a new clawless water-bear (Invertebrata: Tardigrada) from Western Australia. *Journal of the Royal Society of Western Australia* 69 (1): 1–4.

Murray J. 1907. VI. – Some Tardigrada of the Sikhim Himalaya. *Journal of the Royal Microscopical Society* 27 (3): 269–273. https://doi.org/10.1111/j.1365-2818.1907.tb01654.x

Murray J. 1910. Tardigrada. *British Antarctic Expedition 1907–1909. Reports on the Scientific Investigations* 1 (Biology, Part V): 83–187.

Nelson D.R., Guidetti R. & Rebecchi L. 2015. Phylum Tardgrada. *In*: Thorp J.H. & Covich A.P. (eds) *Thorp and Covich's Freshwater Invertebrates*: 347–380. Academic Press. https://doi.org/10.1016/B978-0-12-385026-3.00017-6

Nowak B. & Stec D. 2017. The first record of *Macrobiotus vladimiri* Bertolani, Biserov, Rebecchi and Cesari, 2011 (Tardigrada: Eutardigrada: Macrobiotidae: *hufelandi* group) from Poland. *Turkish Journal of Zoology* 41: 558–567. https://doi.org/10.3906/zoo-1609-22

Nowak B. & Stec D. 2018. An integrative description of *Macrobiotus hannae* sp. nov. (Tardigrada: Eutardigrada: Macrobiotidae: *hufelandi* group) from Poland. *Turkish Journal of Zoology* 42: 269–286. https://doi.org/10.3906/zoo-1712-31

Pilato G. 1981. Analisi di nuovi caratteri nello studio degli Eutardigradi. *Animalia* 8: 51–57.

Pilato G. & Binda M.G. 2010. Definition of families, subfamilies, genera and subgenera of the Eutardigrada, and keys to their identification. *Zootaxa* 2404: 1–52. https://doi.org/10.11646/zootaxa.2404.1.1

Pilato G. & Lisi O. 2004. *Doryphoribius neglectus* sp. n. and *Parascon nichollsae* sp. n., new species of eutardigrades from Australia. *Zootaxa* 545: 1–7. https://doi.org/10.11646/zootaxa.545.1.1

Pilato G., Kiosya Y., Lisi O. & Sabella G. 2012. New records of Eutardigrada from Belarus with the description of three new species. *Zootaxa* 3179: 39–60. https://doi.org/10.11646/zootaxa.3179.1.2

Rambaut A., Drummond A.J., Xie D., Baele G. & Suchard M.A. 2018. Posterior summarization in Bayesian phylogenetics using Tracer 1.7. *Systematic Biology* 67 (5): 901–904. https://doi.org/10.1093/sysbio/syy032

Richters F. 1908. Beitrag zur Kenntnis der Moosfauna Australiens und der Inseln des Pazifischen Ozeans. *Zoologische Jahrbücher, Abteilung für Systematik, Geografie und Biologie der Tiere* 26: 196–213. Available from https://biodiversitylibrary.org/page/27521375 [accessed 22 Oct. 2019].

Roa G.C. 1972. On the zoogeography of the interstitial tardigrade *Parastygarctus higginsi* Renaud-Debyser, 1965 in the intertidal sands on Andaman Islands. *Current Science* 41 (23): 845–846.

Ronquist F. & Huelsenbeck J.P. 2003. MrBayes 3: Bayesian phylogenetic inference under mixed models. *Bioinformatics* 19: 1572–1574. https://doi.org/10.1093/bioinformatics/btg180

Roszkowska M., Ostrowska M., Stec D., Janko K. & Kaczmarek Ł. 2017. *Macrobiotus polypiformis* sp. nov., a new tardigrade (Macrobiotidae; *hufelandi* group) from the Ecuadorian Pacific coast, with remarks on the claw abnormalities in eutardigrades. *European Journal of Taxonomy* 327: 1–19. https://doi.org/10.5852/ejt.2017.327

Roszkowska M., Ostrowska M., Grobys D., Kmita H. & Kaczmarek Ł. 2019. Some tardigrades from Italy, with an updated checklist of limno-terrestrial species from the country. *Acta Zoologica Bulgarica* 71 (2): 167–174.

Schill R.O., Forster F., Dandekar T. & Wolf N. 2010. Using compensatory base change analysis of internal transcribed spacer 2 secondary structures to identify three new species in *Paramacrobiotus* (Tardigrada). *Organisms Diversity & Evolution* 10 (4): 287–296. https://doi.org/10.1007/s13127-010-0025-z

Stec D. & Kristensen R.M. 2017. An integrative description of *Mesobiotus ethiopicus* sp. nov. (Tardigrada: Eutardigrada: Parachela: Macrobiotidae: *harmsworthi* group) from the Northern Afrotropic region. *Turkish Journal of Zoology* 41: 800–811. https://doi.org/10.3906/zoo-1701-47

Stec D., Smolak R., Kaczmarek Ł. & Michalczyk Ł. 2015. An integrative description of *Macrobiotus paulinae* sp. nov. (Tardigrada: Eutardigrada: Macrobiotidae: *hufelandi* group) from Kenya. *Zootaxa* 4052: 501–526. https://doi.org/10.11646/zootaxa.4052.5.1

Stec D., Gąsiorek P., Morek W., Kosztyła P., Zawierucha K., Michno K., Kaczmarek Ł., Prokop Z.M. & Michalczyk Ł. 2016a. Estimating optimal sample size for tardigrade morphometry. *Zoological Journal of the Linnean Society* 178: 776–784. https://doi.org/10.1111/zoj.12404

Stec D., Morek W., Gąsiorek P., Kaczmarek Ł. & Michalczyk Ł. 2016b. Determinants and taxonomic consequences of extreme egg shell variability in *Ramazzottius subanomalus* (Biserov, 1985) (Tardigrada). *Zootaxa* 4208 (2): 176–188. https://doi.org/10.11646/zootaxa.4208.2.5

Stec D., Zawierucha K. & Michalczyk Ł. 2017a. An integrative description of *Ramazzottius subanomalus* (Biserov, 1985) (Tardigrada) from Poland. *Zootaxa* 4300 (3): 403–420. https://doi.org/10.11646/zootaxa.4300.3.4

Stec D., Morek W., Gąsiorek P., Blagden B. & Michalczyk Ł. 2017b. Description of *Macrobiotus scoticus* sp. nov. (Tardigrada: Macrobiotidae: *hufelandi* group) from Scotland by means of integrative taxonomy. *Annales Zoologici* 67: 181–197. https://doi.org/10.3161/00034541ANZ2017.67.2.001

Stec D., Arakawa K. & Michalczyk Ł. 2018a. An integrative description of *Macrobiotus shonaicus* sp. nov. (Tardigrada: Macrobiotidae) from Japan with notes on its phylogenetic position within the *hufelandi* group. *PLoS ONE* 13: e0192210. https://doi.org/10.1371/journal.pone.0192210

Stec D., Krzywański Ł. & Michalczyk Ł. 2018b. Integrative description of *Macrobiotus canaricus* sp. nov. with notes on *M. recens* (Eutardigrada: Macrobiotidae). *European Journal of Taxonomy* 452: 1–36. https://doi.org/10.5852/ejt.2018.452

Stec D., Morek W., Gąsiorek P. & Michalczyk Ł. 2018c. Unmasking hidden species diversity within the *Ramazzottius oberhaeuseri* complex, with an integrative redescription of the nominal species for the family Ramazzottiidae (Tardigrada: Eutardigrada: Parachela). *Systematics and Biodiversity* 16 (4): 357–376. https://doi.org/10.1080/14772000.2018.1424267

Stec D., Kristensen R.M. & Michalczyk Ł. 2018d. Integrative taxonomy identifies *Macrobiotus papei*, a new tardigrade species of the *Macrobiotus hufelandi* complex (Eutardigrada: Macrobiotidae) from the Udzungwa Mountains National Park (Tanzania). *Zootaxa* 4446: 273–291. https://doi.org/10.11646/zootaxa.4446.2.7

Tumanov D.V. 2006. Five new species of the genus *Milnesium* (Tardigrada, Eutardigrada, Milnesiidae). *Zootaxa* 1122: 1–23. https://doi.org/10.11646/zootaxa.1122.1.1

Tumanov D.V. 2018. First data on the freshwater Tardigrada in India: a find of *Pseudobiotus kathmanae* in a small Himalayan lake. *Zoosystematica Rossica* 27 (2): 218–223. https://doi.org/10.31610/zsr/2018.27.2.218

Van Rompu E.A., De Smet W.H. & Coomans A. 1995. Some terrestrial tardigrades from Zimbabwe. *Biologisch Jaarboek* 62: 48–55.

Vecchi M., Ceasri M., Bertolani R., Jönsson K.I., Rebecchi L. & Guidetti R. 2016. Integrative systematic studies on tardigrades from Antarctica identify new genera and new species within Macrobiotoidea and Echiniscoidea. *Invertebrate Systematics* 30 (4): 303–322. https://doi.org/10.1071/IS15033

Wełnicz W., Grohme M.A., Kaczmarek Ł., Schill R.O. & Frohme M. 2011. ITS-2 and 18S rRNA data from *Macrobiotus polonicus* and *Milnesium tardigradum* (Eutardigrada, Tardigrada). *Journal of Zoological Systematics and Evolutionary Research* 49 (S1): 34–39. https://doi.org/10.1111/j.1439-0469.2010.00595.x

Zeller C. 2010. *Untersuchung der Phylogenie von Tardigraden anhand der Genabschnitte 18S rDNA und Cytochrom c Oxidase Untereinheit 1 (COX I).* MSc Thesis, *Technische Hochschule Wildau*, Germany.

*Manuscript received: 6 August 2019*
*Manuscript accepted: 12 September 2019*
*Published on: 31 October 2019*
*Topic editor: Rudy Jocqué*
*Desk editor: Kristiaan Hoedemakers*

Printed versions of all papers are also deposited in the libraries of the institutes that are members of the *EJT* consortium: Muséum national d'histoire naturelle, Paris, France; Meise Botanic Garden, Belgium; Royal Museum for Central Africa, Tervuren, Belgium; Royal Belgian Institute of Natural Sciences, Brussels, Belgium; Natural History Museum of Denmark, Copenhagen, Denmark; Naturalis Biodiversity Center, Leiden, the Netherlands; Museo Nacional de Ciencias Naturales-CSIC, Madrid, Spain; Real Jardín Botánico de Madrid CSIC, Spain; Zoological Research Museum Alexander Koenig, Bonn, Germany; National Museum, Prague, Czech Republic.

## Appendix 1

Sequences of species from the *Macrobiotus hufelandi* group used for molecular comparisons in this study. Underlined GenBank accession numbers indicate type or neotype sequences.

| DNA marker | Species | Accession number | Source |
|---|---|---|---|
| **18S rRNA** | *M. canaricus* Stec *et al.*, 2018 | MH063925 | Stec *et al.* (2018b) |
| | "*M. hufelandi*" Schultze, 1834 | GQ849024 | Giribet *et al.* (1996) |
| | *M. hufelandi* group species | HQ604971, FJ435738–FJ435740 | Bertolani *et al.* (2014), Guil & Giribet (2012) |
| | *M. hannae* Nowak & Stec, 2018 | MH063922 | Nowak & Stec (2018) |
| | "*M. joannae*" Pilato & Binda, 1983 [= *M. hannae* Nowak & Stec, 2018] | HQ604974–5 | Bertolani *et al.* (2014) |
| | *M. kristenseni* Guidetti *et al.*, 2013 | KC193577 | Guidetti *et al.* (2013) |
| | *M. macrocalix* Bertolani & Rebecchi, 1993 | HQ604976 | Bertolani *et al.* (2014) |
| | | MH063926 | Stec *et al.* (2018b) |
| | *M. papei* Stec *et al.*, 2018 | MH063881 | Stec *et al.* (2018d) |
| | *M. paulinae* Stec *et al.*, 2015 | KT935502 | Stec *et al.* (2015) |
| | *M. polypiformis* Roszkowska *et al.*, 2017 | KX810008 | Roszkowska *et al.* (2017) |
| | *M. polonicus* Pilato *et al.*, 2003 | HM187580 | Wełnicz *et al.* (2011) |
| | *M.* cf. *recens* Cuénot, 1932 | MH063927 | Stec *et al.* (2018b) |
| | *M. sapiens* Binda & Pilato, 1984 | DQ839601 | Bertolani *et al.* (2014) |
| | *M. scoticus* Stec *et al.*, 2017 | KY797265 | Stec *et al.* (2017b) |
| | *M. shonaicus* Stec *et al.*, 2018 | MG757132 | Stec *et al.* (2018a) |
| **28S rRNA** | *M. canaricus* Stec *et al.*, 2018 | MH063934 | Stec *et al.* (2018b) |
| | *M. hannae* Nowak & Stec, 2018 | MH063924 | Nowak & Stec (2018) |
| | *M. hufelandi* group species | FJ435751, FJ435754–5 | Guil & Giribet (2012) |
| | *M. macrocalix* Bertolani & Rebecchi, 1993 | MH063935 | Stec *et al.* (2018b) |
| | *M. papei* Stec *et al.*, 2018 | MH063880 | Stec *et al.* (2018d) |
| | *M. paulinae* Stec *et al.*, 2015 | KT935501 | Stec *et al.* (2015) |
| | *M. polypiformis* Roszkowska *et al.*, 2017 | KX810009 | Roszkowska *et al.* (2017) |
| | *M.* cf. *recens* Cuénot, 1932 | MH063936 | Stec *et al.* (2018b) |
| | *M. scoticus* Stec *et al.*, 2017 | KY797266 | Stec *et al.* (2017b) |
| | *M. shonaicus* Stec *et al.*, 2018 | MG757133 | Stec *et al.* (2018a) |

| DNA marker | Species | Accession number | Source |
|---|---|---|---|
| **ITS-2** | *M. canaricus* Stec *et al.*, 2018 | MH063928–30 | Stec *et al.* (2018b) |
| | *M. hannae* Nowak & Stec, 2018 | MH063923 | Nowak & Stec (2018) |
| | *M. macrocalix* Bertolani & Rebecchi, 1993 | MH063931 | Stec *et al.* (2018b) |
| | *M. papei* Stec *et al.*, 2018 | MH063921 | Stec *et al.* (2018d) |
| | *M. paulinae* Stec *et al.*, 2015 | KT935500 | Stec *et al.* (2015) |
| | *M. polonicus* Pilato *et al.*, 2003 | HM150647 | Wełnicz *et al.* (2011) |
| | *M. polypiformis* Roszkowska *et al.*, 2017 | KX810010 | Roszkowska *et al.* (2017) |
| | *M.* cf. *recens* Cuénot, 1932 | MH063932–3 | Stec *et al.* (2018b) |
| | *M. sapiens* Binda & Pilato, 1984 | GQ403680 | Schill *et al.* (2010) |
| | *M. scoticus* Stec *et al.*, 2017 | KY797268 | Stec *et al.* (2017b) |
| | *M. shonaicus* Stec *et al.*, 2018 | MG757134–5 | Stec *et al.* (2018a) |
| **COI** | *M. canaricus* Stec *et al.*, 2018 | MH057765–6 | Stec *et al.* (2018b) |
| | *M. hannae* Nowak & Stec, 2018 | MH057764 | Nowak & Stec (2018) |
| | *M.*cf. *hufelandi* Schultze, 1834 | HQ876589–94, HQ876596 | Bertolani *et al.* (2011a) |
| | *M. hufelandi* Schultze, 1834 | HQ876584, HQ876586–8 | Bertolani *et al.* (2011a) |
| | *M. kristenseni* Guidetti *et al.*, 2013 | KC193575–6 | Guidetti *et al.* (2013) |
| | *M. macrocalix* Bertolani & Rebecchi, 1993 | FJ176203–7, FJ176208–17, HQ876571, MH057767 | Cesari *et al.* (2009), Bertolani *et al.* (2011a), Stec *et al.* (2018b) |
| | *M. papei* Stec *et al.*, 2018 | MH057763 | Stec *et al.* (2018d) |
| | *M. paulinae* Stec *et al.*, 2015 | KT951668 | Stec *et al.* (2015) |
| | *M. polypiformis* Roszkowska *et al.*, 2017 | KX810011–2 | Roszkowska *et al.* (2017) |
| | *M.* cf. *recens* Cuénot, 1932 | MH057768–9 | Stec *et al.* (2018b) |
| | *M. sandrae* Bertolani & Rebecchi, 1993 | HQ876566–67, HQ876569–70, HQ876572–83 | Bertolani *et al.* (2011a) |
| | *M. scoticus* Stec *et al.*, 2017 | KY797267 | Stec *et al.* (2017b) |
| | *M. shonaicus* Stec *et al.*, 2018 | MG757136–7 | Stec *et al.* (2018a) |
| | *M. terminalis* Bertolani & Rebecchi, 1993 | JN673960, AY598775 | Cesari *et al.* (2011), Guidetti *et al.* (2005) |
| | *M. vladimiri* Bertolani *et al.*, 2011 | HM136931–2, HM136933–4, HQ876568 | Bertolani *et al.* (2011a, 2011b) |